

Estimating Optimal Infinite Horizon Dynamic Treatment Regimes via pT-Learning

Wenzhuo Zhou*, Ruoqing Zhu[†] and Annie Qu[‡]

Abstract

Recent advances in mobile health (mHealth) technology provide an effective way to monitor individuals' health statuses and deliver just-in-time personalized interventions. However, the practical use of mHealth technology raises unique challenges to existing methodologies on learning an optimal dynamic treatment regime. Many mHealth applications involve decision-making with large numbers of intervention options and under an infinite time horizon setting where the number of decision stages diverges to infinity. In addition, temporary medication shortages may cause optimal treatments to be unavailable, while it is unclear what alternatives can be used. To address these challenges, we propose a **Proximal Temporal consistency Learning** (pT-Learning) framework to estimate an optimal regime that is adaptively adjusted between deterministic and stochastic sparse policy models. The resulting minimax estimator avoids the *double sampling* issue in the existing algorithms. It can be further simplified and can easily incorporate off-policy data without mismatched distribution corrections. We study theoretical properties of the sparse policy and establish finite-sample bounds on the excess risk and performance error. The proposed method is implemented by our `proximalDTR` package and is evaluated through extensive simulation studies and the OhioT1DM mHealth dataset.

Key words: Precision medicine; Reinforcement learning; Sparse policy; Policy optimization

*Department of Statistics, University of Illinois Urbana-Champaign, Champaign, IL; email: wenzhuo3@illinois.edu;

[†]Department of Statistics, University of Illinois Urbana-Champaign, Champaign, IL; email: rqzhu@illinois.edu;

[‡]Department of Statistics, University of California Irvine, Irvine, CA; email: aqu2@uci.edu.

1 Introduction

Mobile health (mHealth) technology has recently attracted much attention due to mobile devices such as smartphones or wearable devices for tracking physical activities and well-being. It makes real-time communications feasible between health providers and individuals (Sim, 2019). In addition, the mHealth technology can also be used to collect rich longitudinal data for exploring optimal dynamic treatment regimes, which are critical in delivering long-term personalized interventions (Nahum-Shani et al., 2018). For example, the OhioT1DM mHealth study (Marling and Bunescu, 2020) collects eight weeks’ worth of mHealth data for type 1 diabetes patients. All patients are equipped with mobile sensor bands for continuously measuring blood glucose level, insulin dose level, heart rate, carbohydrate intake, etc. This allows us to develop tailored dynamic treatment strategies to manage patients’ blood glucose levels. However, current applications of mHealth technology in clinical use encounter some unique challenges. First, using mHealth technology involves data collection and requires decision-making over a very long period. This is often referred to as the infinite horizon setting. Secondly, most of the mHealth applications aim to provide multi-channel interventions with a large number of treatment combinations (Yang and Van Stee, 2019), or recommend continuous individualized dose levels (Marling and Bunescu, 2020) for maximizing patients’ clinical outcomes. Thirdly, there is an increasing demand for implementing robust dynamic treatment regimes to meet unexpected situations such as temporary shortage of medications or budget constraints in mHealth studies (Rehg et al., 2017). It is essential to design an optimal regime that can provide an alternative optimal or near-optimal treatment option as a backup choice. However, existing statistical methodologies are not well-developed for meeting the challenges mentioned above.

Although there is a rich body of literature on estimating dynamic treatment regimes (Murphy, 2003; Zhao et al., 2015; Shi et al., 2018) over a fixed period (finite horizon), only a limited number of statistical methodologies have been developed for the infinite horizon setting. Ertefaie and Strawderman (2018) proposed a variant of Greedy GQ-learning to estimate optimal regimes. Luckett et al. (2020) proposed V-learning to search for an optimal policy over a pre-specified class of policies. Xu et al. (2020) later extended V-learning to latent space models. Among other

works, [Liao et al. \(2020\)](#), [Uehara et al. \(2020\)](#) and [Shi et al. \(2020\)](#) focus on a target policy or value function evaluation instead of finding an optimal policy. In the computer science field, popular approaches include learning the optimal value function firstly, and then recovering the corresponding optimal policy ([Antos et al., 2008](#); [Dai et al., 2018](#)). Other methods include the residual gradient algorithm ([Baird, 1995](#)) and PCL learning ([Nachum et al., 2017](#); [Chow et al., 2018](#); [Nachum et al., 2018](#)). However, these algorithms encounter the *double sampling* problem ([Sutton and Barto, 2018](#)). Alternatively, entropy-augmented methods ([Schulman et al., 2017](#); [Lee et al., 2018](#); [Haarnoja et al., 2018](#)) follow the principle of developing reinforcement learning algorithms with improved exploration and high robustness. However, their methods are not suitable for continuous state space or large numbers of treatment options.

In this paper, we propose a novel **Proximal Temporal consistency Learning** (pT-Learning) framework for estimating the optimal infinite horizon treatment regime. Through revisiting the standard Bellman equation from an alternative perspective, we construct a proximal counterpart simultaneously addressing the non-smoothness issues and inducing an optimal sparse policy. This distinguishes our method from commonly used approaches in the existing literature. We utilize the path-wise consistency property of the constructed proximal Bellman operator to incorporate off-policy data, and further propose a consistent minimax sample estimator for the optimal policy via leveraging the idea of functional space embedding.

The pT-Learning framework enjoys several unique advantages. Firstly, it shows advantages when the number of treatment options is large and can be easily extended to a continuous treatment space. The induced optimal policy identifies treatments from a sparse subset of the treatment space, indicating that it only assigns (near-)optimal treatment options with nonzero probabilities. Also, this property adaptively adjusts the policy between stochastic and deterministic policy models through a data-driven sparsity parameter, hence bridging the two popular models together. In addition, the induced policy is robust to unexpected situations and guarantees the recommendation of near-optimal treatment alternatives when the optimal treatment is temporarily unavailable. Secondly, the proposed minimax estimator can be directly optimized over the observed sample transition path without the *double sampling* required in existing algo-

rithms. Thirdly, pT-Learning captures the optimal policy and value function jointly over any arbitrary state-action pair. This avoids the mismatched distributions adjustments, e.g., inverse propensity-score weighting in [Lockett et al. \(2020\)](#), for off-policy data. Fourthly, our method intrinsically achieves flexibility in choosing the value function approximation class without the risk of diverging from the optimal solution. In contrast, existing methods such as the Q-learning ([Watkins and Dayan, 1992](#)), Temporal Difference learning ([Dann et al., 2014](#)) and Greedy GQ-learning ([Ertefaie and Strawderman, 2018](#)) may either diverge to infinity in off-policy training or only have guaranteed convergence in linear function space. Lastly, the proposed constrained min-max optimization problem can be reduced to an unconstrained minimization problem, which can be solved under a scalable and efficient unified *actor-critic* framework. This greatly reduces the computational cost and improves the stability of the optimal policy and value function learning.

In addition to these unique advantages, our study makes important contributions to the fundamental problem of solving the Bellman equation when function approximation is used. We provide a substantial development for addressing the decade-long *double sampling* problem in policy optimization. In addition, our approach draws a connection and provides an alternative understanding to the entropy-augmented Markov decision process problem ([Schulman et al., 2017](#); [Lee et al., 2018](#); [Haarnoja et al., 2018](#)). Our method is motivated by addressing the non-smoothness issue of the Bellman equation while inducing policy sparsity. It is fundamentally different from the principles of the existing entropy-augmented methods, which focus on improving exploration ability and algorithmic robustness. In theory, we establish the first theoretical result for the adaptivity of sparse policy distributions. Moreover, we develop finite-sample upper bounds on both the excess risk and the performance error. This is the first non-asymptotic result to quantify the performance error on both deterministic and stochastic policy models jointly, to the best of our knowledge.

2 Background and Notation

First, we introduce the background for the estimating dynamic treatment regime in infinite horizon settings, which can be modeled by the Markov decision process (MDP, [Puterman, 2014](#)). The MDP is denoted as a tuple $(\mathcal{S}, \mathcal{A}, \mathbf{P}, R)$, where \mathcal{S} is a state space, \mathcal{A} is an action (treatment) space, $\mathbf{P}(\cdot|s, a)$ is an unknown Markov transition kernel, and R denotes an immediate utility. A trajectory induced by the MDP can be written as $\mathcal{D} = \{S^1, A^1, S^2, A^2, S^3, \dots, \dots, S^{T+1}\}$, where $S^t \in \mathcal{S}$ is the patient's health state at t , $A^t \in \mathcal{A}$ is the action assignment at t , and T denotes the length of trajectory assumed to be non-random for simplicity. The observed data $\mathcal{D}_n = \{\mathcal{D}_i\}_{i=1}^n$ comprises n independent and identical distributed trajectories of \mathcal{D} . Here, the state evolves following the time-homogenous Markov process. For all $t \geq 1$, $S^{t+1} \perp (S^1, A^1, \dots, S^{t-1}, A^{t-1}) \mid (A^t, S^t)$ and $\mathbf{P}(S^{t+1} = s' | S^t = s, A^t = a) = \mathbf{P}(s' | s, a)$. The immediate utility at t is defined as $R^t = u(S^{t+1}, A^t, S^t) : \mathcal{S} \times \mathcal{A} \times \mathcal{S} \rightarrow \mathbb{R}$, where $u(\cdot)$ is a known function measuring the near-impact of the action A^t . A dynamic treatment regime (policy) $\pi : \mathcal{S} \rightarrow \mathcal{P}(\mathcal{A})$ is a map from the state space \mathcal{S} to the probability distribution simplex over \mathcal{A} .

The discounted sum of utilities beyond the time t is represented as $\sum_{k=1}^{\infty} \gamma^{k-1} R^{t+k}$, where $\gamma \in (0, 1)$ is the discount factor. Our goal is to find a policy π to maximize the expected discounted sum of utilities from time t until death, which is defined as the infinite-horizon value function $V_t^\pi(s) = \mathbb{E} [\sum_{k=1}^{\infty} \gamma^{k-1} R^{t+k} \mid S^t = s]$. The infinite-horizon action-value function $Q_t^\pi(s, a) = \mathbb{E} [\sum_{k=1}^{\infty} \gamma^{k-1} R^{t+k} \mid S^t = s, A^t = a]$ is the same as $V_t^\pi(s)$, except for taking treatment a given the state s at time t and then following π till the end. In the time-homogenous Markov process, $V_t^\pi(s)$ and $Q_t^\pi(s, a)$ do not depend on t ([Sutton and Barto, 2018](#)). The optimal action-value function $Q^*(s, a) = \max_{\pi} Q^\pi(s, a)$ is *unique*, and satisfies the Bellman optimality equation ([Puterman, 2014](#)):

$$Q^*(s, a) = \mathbb{E}_{S^{t+1}|s, a} \left[R^t + \gamma \max_{\bar{a} \in \mathcal{A}} Q^*(S^{t+1}, \bar{a}) \mid S^t = s, A^t = a \right], \quad (2.1)$$

where $\mathbb{E}_{S^{t+1}|s, a}$ is a short notation for $\mathbb{E}_{S^{t+1} \sim \mathbf{P}(S^{t+1}|s, a)}$. A policy π^* satisfying the equation $Q^*(s, a) = Q^{\pi^*}(s, a)$ is referred to as an optimal policy, but it might not be unique. An optimal policy $\pi^* = \bar{\pi}$ can be obtained by taking the *greedy* action of $Q^*(s, a)$, where $\bar{\pi} \in$

$\arg \max_a Q^*(s, a)$. We define the Bellman operator \mathcal{B} as

$$\mathcal{B}V(s) := \max_{a \in \mathcal{A}} \mathbb{E}_{S^{t+1}|s,a} [R^t + \gamma V(S^{t+1}) \mid S^t = s, A^t = a]. \quad (2.2)$$

Then $V^{\bar{\pi}}(s)$ is the unique fixed point of \mathcal{B} such that $\mathcal{B}V^{\bar{\pi}} = V^{\bar{\pi}}$.

3 Methodology

To develop the new framework, we introduce a proximal Bellman operator and the associated sparse and adaptive optimal policy in Section 3.1. To estimate such an optimal policy, we propose a minimax framework called proximal temporal consistency learning in Section 3.2. The proposed method is theoretically guaranteed, and is also practical for addressing the challenges in mHealth applications.

The *greedy* optimal policy $\bar{\pi} \in \arg \max_a Q^*(s, a)$ in (2.1) is a deterministic policy, which recommends an action instead of a probability distribution, given a state. In practice, a deterministic policy might not be robust for unexpected situations whenever the true optimal action is temporarily unavailable or difficult to implement. In contrast, a stochastic policy usually characterizes the optimal decision rule by a probability distribution, which provides a probability of suggesting other near-optimal actions in addition to the optimal one. In the existing literature, many works use the Boltzmann distribution to model the optimal policy distribution (Schulman et al., 2017; Haarnoja et al., 2018; Lockett et al., 2020). However, such a policy distribution is prone to assigning nonzero probability mass to all actions, including non-optimal and dismissible ones. This could be problematic when the cardinality of the action space is large, which may cause the policy distribution to degenerate to a uniform distribution, and potentially fails to provide a desired action recommendation.

These challenges motivate us to develop an optimal policy following a distribution whose support set is a sparse subset of the action space containing only (near-)optimal actions. We refer to this class of policies as the *sparse* policy. Specially, the deterministic policy $\bar{\pi}$ can be viewed as the most extreme case of sparse policies and inherits some advantages of the

sparse policies. However, the deterministic policy $\bar{\pi}$ always takes a greedy action, resulting in potential sub-optimality, and cannot deal with unexpected situations such as temporary shortages of medications or budget constraints. In this paper, we aim to design and estimate an optimal policy that enjoys policy sparsity while inheriting the advantages of the stochastic policy model.

To start with, we first revisit the Bellman optimality equation in (2.2) from a policy-explicit view. Suppose the policy π follows a stochastic distribution, then the Bellman optimality equation can be reformulated as

$$\mathcal{B}V(s) := \max_{\pi} \mathbb{E}_{a \sim \pi(\cdot|s), S^{t+1}|s,a} [u(S^{t+1}, s, a) + \gamma V(S^{t+1})] = V(s), \quad (3.1)$$

To solve the above equation (3.1), a natural idea is to jointly optimize V and π to minimize the difference between $\mathcal{B}V(s)$ and $V(s)$ for any s . However, the equation (3.1) is nonlinear and contains a non-smooth *max* operator. When either the state space \mathcal{S} or action space \mathcal{A} is large, directly solving (3.1) often results in policies that are far from the optimal solution. In addition, the discontinuity and instability caused by the *max* operator make estimation very difficult without large amounts of samples. To address these issues, we need to consider a proximal counterpart of the Bellman equation (3.1).

3.1 Proximal Bellman Operator

In this section, we propose a proximal Bellman operator that circumvents the obstacles of solving (3.1), while simultaneously inducing an adaptive and sparse optimal policy. The proposed framework bridges the gap between the deterministic and stochastic policy models and characterizes the intrinsic relationship between the two policy models.

Let $\mathcal{P}(\mathcal{A})$ be a convex probability simplex over \mathcal{A} ; we reformulate the Bellman operator \mathcal{B} under the Fenchel representation, that is

$$\mathcal{B}V(s) = \max_{\pi \in \mathcal{P}(\mathcal{A})} \sum_{a \in \mathcal{A}} \left[\langle \mathbb{E}_{S^{t+1}|s,a} [u(S^{t+1}, s, a) + \gamma V(S^{t+1})], \pi(a|s) \rangle - \mu(\pi(a|s)) \right], \quad (3.2)$$

where $\langle \cdot, \cdot \rangle$ denotes the dot product and $\mu(\cdot)$ is a constant function always equals to zero in our case. The representation (3.2) provides a basis for constructing a proximity of $\mathcal{B}V(s)$. Specifically,

we consider to add a strongly convex and continuous component $d(\pi) : \mathcal{P}(\mathcal{A}) \rightarrow \mathbb{R}$ to the dual of (3.2):

$$\begin{aligned} \mathcal{B}_\lambda V_\lambda(s) &= \max_{\pi \in \mathcal{P}(\mathcal{A})} \sum_{a \in \mathcal{A}} \left[\langle \mathbb{E}_{S^{t+1} \sim p(\cdot|s,a)} [u(S^{t+1}, s, a) + \gamma V_\lambda(S^{t+1})], \pi(a|s) \rangle - \mu(\pi(a|s)) + \lambda d(\pi(a|s)) \right] \\ &= \max_{\pi \in \mathcal{P}(\mathcal{A})} \mathbb{E}_{a \sim \pi(\cdot|s)} \left[Q_\lambda(s, a) + \lambda \phi(\pi(a|s)) \right], \end{aligned} \quad (3.3)$$

where $\phi(x) = d(x)/x$ with the proximity function $d(\cdot)$ and $Q_\lambda(s, a) := \mathbb{E}_{S^{t+1}|s,a} [u(S^{t+1}, s, a) + \gamma V_\lambda(S^{t+1})]$. By the Fenchel transformation theorem, the proximity $\mathcal{B}_\lambda V_\lambda(s)$ is a smooth approximation for $\mathcal{B}V(s)$ if some conditions on the proximity function $d(\cdot)$ are satisfied (Hiriart-Urruty and Lemaréchal, 2012).

Here, we should notice that we are not satisfied with only achieving the smoothing purpose but aim to develop a sparse optimal policy. To achieve this goal, we define a class of proximity functions based on the κ -logarithm function (Korbel et al., 2019), i.e., $d(x) = x\phi(x) = -\frac{x}{2} \log_\kappa(x)$, where $\log_\kappa(x) = \frac{1}{1-\kappa} (x^{1-\kappa} - 1)$ for $x > 0$ and $\kappa \neq 1$. In this paper, we consider a special case when $k = 0$, and refer to the operator (3.3) as the *proximal Bellman operator*.

Accordingly, the proximal Bellman operator (3.3) has several unique properties. First, it is a valid approximation for the Bellman operator \mathcal{B} , where the approximation bias is bounded in Theorem S.1 in the Appendix. Second, it is a smooth substitute of \mathcal{B} according to the closed form of \mathcal{B}_λ in (3.4). Third, the proximal Bellman operator \mathcal{B}_λ induces a sparse optimal policy whose sparsity can be adjusted by the magnitude of λ .

Specifically, through verifying the KKT conditions of the maximization in (3.3), the proximal Bellman operator \mathcal{B}_λ has a closed-form equivalence (see Proposition S.1 in the Appendix):

$$\mathcal{B}_\lambda V_\lambda(s) = \frac{\lambda}{2} \left\{ 1 - \sum_{a \in \mathcal{K}(s)} \left[\left(\frac{\sum_{a \in \mathcal{K}(s)} Q_\lambda(s, a)}{\lambda |\mathcal{K}(s)|} - \frac{1}{|\mathcal{K}(s)|} \right)^2 - \left(\frac{Q_\lambda(s, a)}{\lambda} \right)^2 \right] \right\}, \quad (3.4)$$

where $|\cdot|$ denotes the cardinality of a set and $\mathcal{K}(s)$ represents the support action set at state s , that is $\mathcal{K}(s) = \{a_{(i)} \in \mathcal{A} : Q_\lambda(s, a_{(i)}) > \frac{1}{i} \sum_{j=1}^i Q_\lambda(s, a_{(j)}) - \frac{\lambda}{i}\}$. Here $a_{(i)}$ is the action with the i -th largest state-action value, and $|\mathcal{K}(s)| \leq |\mathcal{A}|$ always holds for any $s \in \mathcal{S}$.

The proximal Bellman operator (3.4) does not involve the *max* operator and being differen-

tiable everywhere, and the degree of smoothness is determined by the magnitude of λ according to Proposition S.1. We visualize this property in Figure 1 under a binary action setting. As λ increases, the proximal Bellman operator \mathcal{B}_λ becomes a more smooth approximation of \mathcal{B} but the approximation bias increases accordingly, indicating that the parameter λ controls the bias and smoothness trade-off.

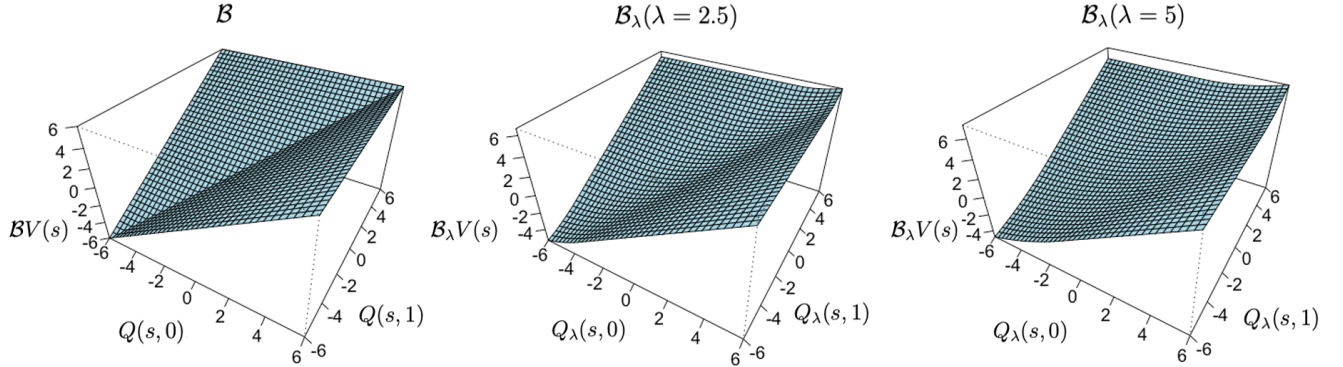


Figure 1: Comparison of the standard Bellman operator $\mathcal{B}V(s)$ and the proximal Bellman operator $\mathcal{B}_\lambda V(s)$ with $\lambda = 2.5$ and $\lambda = 5$ in a binary action setting.

In addition to the smoothness property, the proximal Bellman operator \mathcal{B}_λ induces a sparse optimal policy distribution $\pi_\lambda(a|s)$ whose support set is a sparse subset of the action space. We illustrate this point by presenting $\pi_\lambda(a|s)$ in terms of the state-action value function $Q_\lambda(s, a)$ analytically (see the proof of Proposition S.1). That is

$$\pi_\lambda(a|s) = \left(\frac{Q_\lambda(s, a)}{\lambda} - \frac{\sum_{a \in \mathcal{K}(s)} Q_\lambda(s, a)}{\lambda |\mathcal{K}(s)|} + \frac{1}{|\mathcal{K}(s)|} \right)^+. \quad (3.5)$$

Given any state s , the equation (3.5) gives a well-defined probability mass function in that $\sum_{a \in \mathcal{A}} \pi_\lambda(a|s) = 1$. Also, the policy $\pi_\lambda(a|s)$ is prone to assign a large probability to the action according to the rank of the state-action values. This ensures that the policy $\pi_\lambda(a|s)$ can recommend the optimal action in any state.

Moreover, sparsity can be shown by analyzing the support set of $\pi_\lambda(\cdot|s)$, i.e., $\{a \in \mathcal{A} : \pi_\lambda(a|s) > 0\}$, which satisfies

$$\left\{ a_{(i)} \in \mathcal{A} : Q_\lambda(s, a_{(i)}) > \frac{1}{i} \sum_{j=1}^i Q_\lambda(s, a_{(j)}) - \frac{\lambda}{i} \right\}. \quad (3.6)$$

The inequality (3.6) indicates that the sparsity parameter λ controls the margins between the smallest action value and the others included in the support set (3.6). In particular, the cardinality of the support set increases as λ increases. Conversely, the support set of $\pi_\lambda(\cdot|s)$ shrinks as λ becomes smaller. To illustrate how this mechanism works, we use a ternary action setting as an example. By the inequality (3.6), when λ is sufficiently small in that $\lambda < Q_\lambda(s, a_{(1)}) - Q_\lambda(s, a_{(2)})$, only $a_{(1)}$ is contained in the support set. The policy distribution becomes a deterministic rule and takes the greedy action with the largest action value $Q_\lambda(s, a_{(1)})$. In this point of view, the Q-learning approach and its variants can be regarded as special cases in our framework. If λ increases and falls into the range $[Q_\lambda(s, a_{(1)}) - Q_\lambda(s, a_{(2)}), \sum_{i=1}^2 Q_\lambda(s, a_{(i)}) - 2Q_\lambda(s, a_{(3)})]$, the support set contains two actions $a_{(1)}$ and $a_{(2)}$ with the largest state-action values, but eliminates action $a_{(3)}$. This implies that the induced policy can be adaptively adjusted between the deterministic and stochastic policy models. In Section 4, we investigate the sparsity of the optimal policy distribution with more detail.

3.2 Proximal Temporal Consistency Learning

Next, we introduce the proposed proximal temporal consistency learning framework for estimating the induced optimal policy π_λ . Our development mainly hinges on a path-wise property of the proximal Bellman operator \mathcal{B}_λ and the functional space embedding (Gretton et al., 2012). The proposed minimax estimator is able to address the *double sampling* issue and easily incorporate off-policy data, while intrinsically preserving the convergence in off-policy training with flexible function approximations.

First, we show that the proximal Bellman operator \mathcal{B}_λ enjoys the temporary consistency property (Rawlik et al., 2013). Most recently, many state-the-art methods based on this type of property have achieved great success in real-life applications (Nachum et al., 2017; Chow et al., 2018; Nachum et al., 2018). The temporary consistency property connects the optimal policy and value function in one equation along with any arbitrary state-action pair, which provides an elegant way to incorporate off-policy data. We present the temporary consistency property for \mathcal{B}_λ in the following proposition.

Proposition 3.1. For any $s \in \mathcal{S}, a \in \mathcal{A}$ and $\lambda \in (0, +\infty)$, if V_λ^* is a fixed point of the equation (3.3), and π_λ^* is the induced policy following the equation (3.5), then $(V_\lambda^*, \pi_\lambda^*)$ is a solution of the following proximal temporal consistency equation:

$$\mathbb{E}_{S^{t+1}|s,a} [u(S^{t+1}, s, a) + \gamma V_\lambda(S^{t+1})] - \lambda \phi(\pi_\lambda(a|s)) - \Psi(s) + \psi(a|s) - V_\lambda(s) = 0, \quad (3.7)$$

where $\Psi(s) : \mathcal{S} \rightarrow [-\lambda/2, 0]$ and $\psi(a|s) : \mathcal{S} \times \mathcal{A} \rightarrow \mathbb{R}^+$ are Lagrangian multipliers with $\psi(a|s) \cdot \pi_\lambda(a|s) = 0$, and we call the discrepancy on the left-hand side of the equation (3.7) the proximal temporary consistency error (pT-error).

Since the equation (3.7) holds for any arbitrary state-action pair (s, a) , the policy π_λ can be estimated directly over the observed transition pairs. Utilizing this property lets us skip to adjust mismatched distributions using, e.g., inverse propensity-score weighting (Luckett et al., 2020), and avoids the curse of high variance (Jiang and Li, 2016) carried over from the data distribution corrections. To solve the equation (3.7), an intuitive idea is to minimize the pT-error with the L^2 loss,

$$\min_{V_\lambda, \pi_\lambda, \Psi, \psi} \mathbb{E}_{S^t, A^t} \left[(\mathcal{T}_{\pi_\lambda}(S^t, A^t, V_\lambda) - \Psi(S^t) + \psi(A^t|S^t) - V_\lambda(S^t))^2 \right] \quad (3.8)$$

$$\text{s.t. } \pi_\lambda(A^t|S^t) \cdot \psi(A^t|S^t) = 0 \text{ and } -\lambda/2 \leq \Psi(S^t) \leq 0, \quad (3.9)$$

where $\mathcal{T}_{\pi_\lambda}(S^t, A^t, V_\lambda) = \mathbb{E}_{S^{t+1}|S^t, A^t} [u(S^{t+1}, S^t, A^t)] + \gamma V_\lambda(S^{t+1})] - \phi(\pi_\lambda(A^t|S^t))$ and \mathbb{E}_{S^t, A^t} is a short notation for $\mathbb{E}_{\{S^t, A^t\} \sim d_{\pi_b}}$ with the observed data distribution d_{π_b} .

However, directly minimizing the sample version of (3.8) is not realizable, as the conditional expectation $\mathbb{E}_{S^{t+1}|S^t, A^t}$ in $\mathcal{T}_{\pi_\lambda}(S_i^t, A_i^t, V_\lambda)$ is unknown. To approximate this unknown expectation, bootstrapping can be applied but produces an inconsistent and biased sample estimator. Specifically, an extra conditional variance $\mathbb{E}_{s \sim d_{\pi_b}} [\text{Var}(R_i^t + \gamma V_\lambda(s)|s)]$ will be involved as a bias component. This problem is usually referred to as the *double-sampling* issue (Baird, 1995) and exists in many policy optimization approaches.

To avoid the *double-sampling* bias, we consider embedding a Lebesgue measurable function class to the averaged pT-error. In particular, we define a critic $h \in \mathcal{H} = L^2(\mathcal{S} \times \mathcal{A})$ and formulate

a novel embedding loss $\mathcal{L}_{\text{weight}}$ as follows,

$$\mathcal{L}_{\text{weight}}(V_\lambda, \pi_\lambda, \Psi, \psi, h) := \mathbb{E}_{S^t, A^t} [h(S^t, A^t) (\mathcal{T}_{\pi_\lambda}(S^t, A^t, V_\lambda) - \Psi(S^t) + \psi(A^t|S^t) - V_\lambda(S^t))]. \quad (3.10)$$

The *critic* function is introduced here to fit the discrepancy of (3.7) and promotes those sampled transition pairs with large pT-error. Unlike the naive L^2 loss (3.8), the nested conditional expectation $\mathbb{E}_{S^{t+1}|S^t, A^t}$ in $\mathcal{T}_{\pi_\lambda}(S^t, A^t, V_\lambda)$ is not inside the square function anymore. Intuitively, the embedding loss circumvents the *double sampling* issue since the second order moment of bootstrapping samples is not involved anymore and the extra condition variance vanishes. Fundamentally, the embedding loss $\mathcal{L}_{\text{weight}}$ offers compensation for insufficient sampling on $\mathbf{P}(s'|s, a)$. The marginal information of the state-action pairs $d_{\pi_b}(s, a)$ and the transition kernel $\mathbf{P}(s'|s, a)$ can be aggregated as a joint distribution $p_{\pi_b}(s', s, a)$ by the linearity of the expectation. Instead of extracting the information from the transition kernel $\mathbf{P}(s'|s, a)$, i.e. approximating the conditional expectation $\mathbb{E}_{S^{t+1}|S^t, A^t}$, the embedding loss can be approximated using the sample-path transition pairs drawn from the joint distribution $p_{\pi_b}(s', s, a)$. In essence, this explains why the embedding loss $\mathcal{L}_{\text{weight}}$ can address the *double sampling* issue.

In the following theorem, we proceed to show $\mathcal{L}_{\text{weight}}(V_\lambda, \pi_\lambda, \Psi, \psi, h)$ is a valid loss which can identify the optimal value function and optimal policy $(V_\lambda^*, \pi_\lambda^*)$. Let $(V_\lambda^*, \pi_\lambda^*)$ be a solution of the equation (3.1), there must exist two Lagrange multipliers Ψ, ψ such that $\mathcal{L}_{\text{weight}}(V_\lambda^*, \pi_\lambda^*, \Psi, \psi, h) = 0$; and the reverse also holds.

Theorem 3.1. *Suppose $\mathcal{S} \times \mathcal{A}$ is Lebesgue measurable, for any $h(\cdot)$ in a bounded L^2 space, i.e., $h(\cdot) \in \mathcal{H}_{L^2}^\zeta := \{h : \|h\|_{L^2} \leq \zeta\}$ for $\zeta \in (0, +\infty)$, the loss function $\mathcal{L}_{\text{weight}}(V_\lambda^*, \pi_\lambda^*, \Psi, \psi, h) = 0$. Furthermore, if there exists $\tilde{V}_\lambda, \tilde{\pi}_\lambda$ such that $\mathcal{L}_{\text{weight}}(\tilde{V}_\lambda, \tilde{\pi}_\lambda, \Psi, \psi, h) = 0$, then $(\tilde{V}_\lambda, \tilde{\pi}_\lambda)$ satisfies the proximal temporary consistency equation (3.7).*

Noticing that $\mathcal{L}_{\text{weight}}(V_\lambda^*, \pi_\lambda^*, \Psi, \psi, h) = 0$ holds for any $h \in \mathcal{H}_{L^2}^\zeta$, Theorem 3.1 immediately leads to a minimax optimization problem,

$$\min_{V_\lambda, \pi_\lambda, \Psi, \psi} \max_{h \in \mathcal{H}_{L^2}^\zeta} \mathcal{L}_{\text{weight}}^2(V_\lambda, \pi_\lambda, \Psi, \psi, h). \quad (3.11)$$

The minimax optimization of (3.11) gives a clear direction to estimating $(V_\lambda^*, \pi_\lambda^*)$, but it still remains intractable. As *critic* function $h(\cdot)$ could be any arbitrary function in $\mathcal{H}_{L^2}^\zeta$, it makes infeasible to find a proper representation for $h(\cdot)$. In the following, we introduce a tractable framework for (3.11) where $h(\cdot)$ can be appropriately represented. For the functions $(V_\lambda, \pi_\lambda, \Psi, \psi)$, we let $h^* : \mathcal{S} \times \mathcal{A} \rightarrow \mathbb{R}$ be an optimal *critic* function if it satisfies

$$h^*(\cdot) \in \arg \max_{h \in \mathcal{H}_{L^2}^\zeta} \mathcal{L}_{\text{weight}}^2(V_\lambda, \pi_\lambda, \Psi, \psi, h). \quad (3.12)$$

In the following, we show that $h^*(\cdot)$ must belong to a class of continuous functions under some regularity continuity conditions which are easily satisfied in practice.

Theorem 3.2. *Let $\mathbb{C}(\mathcal{S} \times \mathcal{A})$ be all continuous functions on $\mathcal{S} \times \mathcal{A}$. For any $(s, a) \in \mathcal{S} \times \mathcal{A}$ and $s' \in \mathcal{S}$, the optimal critic function $h^*(s, a)$ has the following properties:*

1. *(Continuity) Suppose the utility function $u(s', s, a)$ and the transition kernel $\mathbf{P}(s'|s, a)$ are continuous over (s, a) for any s' , then $h^* \in \mathcal{H}_{L^2}^\zeta \cap \mathbb{C}(\mathcal{S} \times \mathcal{A})$ and is unique.*
2. *(Lipschitz-continuity) Suppose $u(s', s, a)$ is uniformly M_u -Lipschitz continuous and $\mathbf{P}(s'|s, a)$ is M_p -Lipschitz continuous over (s, a) for any s' , where M_u and M_p are Lipschitz constants. Then $h^*(s, a)$ is also Lipschitz continuous over (s, a) for the Lipschitz constant M_{h^*} .*

Theorem 3.2 states that the optimal *critic* function $h^*(s, a)$ is continuous over (s, a) if only the utility function and the transition kernel are continuous. This continuity condition widely holds for precision medicine and reinforcement learning problems. As we mentioned, h^* could be any arbitrary function in $\mathcal{H}_{L^2}^\zeta$, which imposes exceptional difficulty in the representation of h^* . Theorem 3.2 indicates that it is sufficient to represent $h(\cdot)$ in a bounded continuous function space, which is tractable and still preserves the optimal solution of (3.11). This provides us a basis for constructing a tractable framework for solving (3.11).

We propose to represent h^* in a bounded reproducing kernel Hilbert space (RKHS) such that $\mathcal{H}_{\mathcal{K}}^\zeta := \{h : \|h\|_{\mathcal{H}_{\text{RKHS}}}^2 \leq \zeta\}$. When $\mathcal{H}_{\mathcal{K}}^\zeta$ is reproduced by a universal kernel, the error $\text{err}(\zeta) := \sup_{f \in \mathbb{C}(\mathcal{S} \times \mathcal{A})} \inf_{h \in \mathcal{H}_{\mathcal{K}}^\zeta} \|f - h\|_\infty$ decreases as ζ increases and vanishes to zero as ζ goes to infinity (Bach, 2017). Therefore, any continuous function can be approximated by a function in $\mathcal{H}_{\mathcal{K}}^\zeta$ with arbitrarily small error. As a result, solving (3.11) over $h^* \in \mathcal{H}_{\mathcal{K}}^\zeta$ turns to be tractable

when $h^* \in \mathcal{H}_{\mathcal{K}}^{\zeta}$.

Note that solving the minimax optimization is still a challenging task. Here, we transform the minimax optimization to an easier solvable minimization problem, leveraging the idea of the kernel embedding (Gretton et al., 2012).

Theorem 3.3. *Suppose $h^* \in \mathcal{H}_{\mathcal{K}}^{\zeta}$ is reproduced by a universal kernel $K(\cdot, \cdot)$, then the minimax optimization (3.11) can be decoupled to a single-stage minimization problem wherein*

$$\min_{V_{\lambda}, \pi_{\lambda}, \Psi, \psi} \mathcal{L}_U = \mathbb{E}_{S^t, \tilde{S}^t, A^t, \tilde{A}^t, S^{t+1}, \tilde{S}^{t+1}} \left[\left(\tilde{\mathcal{T}}_{\pi_{\lambda}}(S^t, A^t, V_{\lambda}) - \Psi(S^t) + \psi(A^t|S^t) - V_{\lambda}(S^t) \right) \cdot \zeta K(\{S^t, A^t\}, \{\tilde{S}^t, \tilde{A}^t\}) \left(\tilde{\mathcal{T}}_{\pi_{\lambda}}(\tilde{S}^t, \tilde{A}^t, V_{\lambda}) - \Psi(\tilde{S}^t) + \psi(\tilde{A}^t|\tilde{S}^t) - V_{\lambda}(\tilde{S}^t) \right) \right], \quad (3.13)$$

where $\tilde{\mathcal{T}}_{\pi_{\lambda}}(S^t, A^t, V_{\lambda}) = u(S^{t+1}, S^t, A^t) + \gamma V_{\lambda}(S^{t+1}) - \phi(\pi_{\lambda}(A^t|S^t))$ and $(\tilde{S}^t, \tilde{A}^t, \tilde{S}^{t+1})$ is an independent copy of the transition pair (S^t, A^t, S^{t+1}) .

Moreover, if the universal kernel $K(\cdot, \cdot)$ is strictly positive definite such that

$$\iint_{\mathcal{S} \times \mathcal{A}} K(\{s, a\}, \{\tilde{s}, \tilde{a}\}) g(\{s, a\}) g(\{\tilde{s}, \tilde{a}\}) d(\{s, a\}) d(\{\tilde{s}, \tilde{a}\}) > 0,$$

for all $g(\cdot, \cdot) \in L^2(\mathcal{S} \times \mathcal{A})$ except for $g(\cdot, \cdot) = 0$, the loss function \mathcal{L}_U is non-negative definite. This implies that $\mathcal{L}_U = 0$ if and only if $(V_{\lambda}, \pi_{\lambda}) = (V_{\lambda}^*, \pi_{\lambda}^*)$. The loss function \mathcal{L}_U is thus a valid loss and can uniquely identify $(V_{\lambda}^*, \pi_{\lambda}^*)$.

Given the observed data \mathcal{D}_n with the length of trajectory T , to minimize \mathcal{L}_U under the constraints in (3.9), we propose a trajectory-based U-statistic estimator to capture the within-trajectory loss. Subsequently, the total loss \mathcal{L}_U can be aggregated as the empirical mean of n *i.i.d.* within-trajectory loss. That is,

$$\begin{aligned} \min_{V_{\lambda}, \pi_{\lambda}, \Psi, \psi} \widehat{\mathcal{L}}_U &= \frac{1}{n} \sum_{i=1}^n \frac{2\zeta}{T(T-1)} \sum_{1 \leq j \neq k \leq T} \left[\left(\tilde{\mathcal{T}}_{\pi_{\lambda}}(S_i^j, A_i^j, V_{\lambda}) - \Psi(S_i^j) + \psi(A_i^j|S_i^j) - V_{\lambda}(S_i^j) \right) \right. \\ &\quad \left. \cdot K(\{S_i^j, A_i^j\}, \{S_i^k, A_i^k\}) \left(\tilde{\mathcal{T}}_{\pi_{\lambda}}(S_i^k, A_i^k, V_{\lambda}) - \Psi(S_i^k) + \psi(A_i^k|S_i^k) - V_{\lambda}(S_i^k) \right) \right]. \\ \text{s.t. } &\pi_{\lambda}(A_i^t|S_i^t) \cdot \psi(A_i^t|S_i^t) = 0 \text{ and } -\lambda/2 \leq \Psi(S_i^t) \leq 0 \text{ for } i = 1, \dots, n; t = 1, \dots, T. \end{aligned} \quad (3.14)$$

Unlike the inconsistent sample estimator in (3.8), the proposed sample estimator $\widehat{\mathcal{L}}_U$ is consistent. The consistency is shown in Theorem 4.2 in Section 4, by examining the tail behavior

of $\widehat{\mathcal{L}}_U$. In addition, the gradient of the proposed loss $\widehat{\mathcal{L}}_U$ can be approximated by the sampled transitions and optimized using any gradient descent type of algorithm. Hence, the proposed method achieves great flexibility in the function approximations of $(V_\lambda^*, \pi_\lambda^*)$, allowing both linear and nonlinear approximations without the risk of divergence from the optimal solution. In comparison, popular methods, including the Q-learning (Watkins and Dayan, 1992), TD-learning (Dann et al., 2014) and Greedy GQ-learning (Maei et al., 2010; Ertefaie and Strawderman, 2018), either diverge to infinity in off-policy training or have guaranteed convergence only in using linear function approximations. Also, we should note that the pT-Learning framework connects to the importance weighted variants of off-policy TD-learning algorithms when the *critic* function $h(\cdot)$ is restricted into a bounded linear function space. We provide a discussion on this connection in the Appendix.

4 Theory

In this section, we establish the theoretical properties of the pT-Learning framework. Our study mainly focuses on three major parts. In the first part, we formally study the sparsity of the policy distribution π_λ . Theorem 4.1 shows that the cardinality of the nonzero probability set for π_λ is well-controlled by the magnitude of λ , which implies that π_λ is adaptively adjusted between the deterministic and stochastic policy models. We believe this is the first theoretical result on investigating the sparsity of policy distributions. In the second part, we establish a convergence rate of the empirical risk $\widehat{\mathcal{L}}_U$ towards the true risk \mathcal{L}_U . In particular, Theorem 4.2 provides a sharp exponential concentration bound, indicating that $\widehat{\mathcal{L}}_U$ is a consistent estimate for \mathcal{L}_U and the *double sample* issue is solved. In the last part, we measure the excess risk of $\widehat{\mathcal{L}}_U$ which is applicable for both the parametric and nonparametric function spaces in Theorem 4.3. Furthermore, Theorem 4.4 provides a finite-sample upper bound on the performance of the estimated optimal value function. The bound indicates both the excess risk and the approximation bias of the proximal Bellman operator will affect the performance error. To the best of our knowledge, this is the first non-asymptotic result to quantify the performance error on determin-

istic and stochastic policy models jointly. In the following, we present our major assumptions and theorems. The proofs and additional theoretical results and assumptions are deferred to the Appendix.

First, we define a notation called Δ -sparsity to characterize the cardinality of nonzero probability actions for any given policy $\pi(\cdot)$.

Definition 4.1. *For all $s \in \mathcal{S}$ and any $a \in \mathcal{A}$, if a policy $\pi(a|s)$ satisfies the condition that $\Delta := \max_{s \in \mathcal{S}} |\{a \in \mathcal{A} : \pi(a|s) \neq 0\}|$ where $|\cdot|$ is the cardinality of a set. The policy $\pi(a|s)$ can be called a Δ -degree sparse policy distribution.*

Theorem 4.1. *Under Assumption S.1-S.2, for any $s \in \mathcal{S}$ and $a \in \mathcal{A}$, let the policy $\pi(a|s) = \pi_\lambda(a|s)$ in (3.5) correspond to the state-action function $Q_\lambda(s, a)$, then $\Delta \rightarrow 1$ as $\lambda \rightarrow 0$, and $\Delta \rightarrow |\mathcal{A}|$ as $\lambda \rightarrow \infty$. In particular, for any $\epsilon > 0$, there exists a positive number λ_0 such that for all $\lambda \geq \lambda_0$, the policy $\pi(a|s)$ approaches a uniform distribution \mathcal{U} , i.e., $|\pi_\lambda(a|s) - |\mathcal{A}|^{-1}| < \epsilon$.*

Theorem 4.1 shows that the degree of sparseness, or the cardinality of the nonzero probability actions, of the policy $\pi_\lambda(\cdot|s)$ can be controlled by λ . In the most extreme case, when $\lambda \rightarrow 0$ such that the sparsity is very certain, the policy π_λ becomes a deterministic policy. Alternatively, as $\lambda \rightarrow +\infty$, the induced policy π_λ degenerates to a uniform distribution that assigns equal probabilities to all action arms.

Before we present the rest of the theoretical results, we need to introduce the stationarity and dependency of the stochastic process $\{(S^t, A^t)\}_{t \geq 1}$. For each single patient trajectory, it is easily observed that the sequence $\{(S^t, A^t)\}_{t \geq 1}$ is a stationary Markov chain. In terms of sample dependency, Farahmand et al. (2016) and Liao et al. (2020) assume that within-trajectory samples are independent in order to reduce technical difficulties in the theoretical developments. However, this assumption might be too restrictive and often violated in practice. In our work, we consider the sample dependency and establish more rigorous theoretical results under the notion of the mixing process (Kosorok, 2008). Specifically, for any stationary sequence of dependent random variables $\{S^t, A^t\}_{t \geq 1}$, let \mathcal{F}_b^c be the σ -field generated by $\{S^b, A^b\}, \dots, \{S^c, A^c\}$ and define $\beta(k) = \mathbb{E} [\sup_{m \geq 1} \{|P(B | \mathcal{F}_1^m) - P(B)| : B \in \mathcal{F}_{m+k}^\infty\}]$, and we say that the process $\{S^t, A^t\}_{t \geq 1}$

is β -mixing if $\beta(k) \rightarrow 0$ as $k \rightarrow \infty$. In the following, we assume a mixing condition to quantify the within-trajectory sample dependency.

Assumption 1. For a strictly stationary sequence $\{(S^t, A^t)\}_{t \geq 1}$, there exists a constant $\delta_1 > 0$ such that the β -mixing coefficient corresponding to $\{(S^t, A^t)\}_{t \geq 1}$ satisfies $\beta(k) \lesssim \exp(-\delta_1 k)$ for $k \geq 1$.

Assumption 2. The immediate utility function $u(S^{t+1}, A^t, S^t)$ is uniformly bounded by R_{\max} , i.e. $\|u\|_\infty \leq R_{\max} < \infty$.

Assumption 1 implies an exponential decay rate of the mixing process, which is typically for deriving a polynomial decay rate of the estimation error (Kosorok, 2008). Assumption 2 is a regular assumption to impose a boundedness condition on the MDP (Antos et al., 2008; Liao et al., 2020).

In Theorem 4.2, we study the tail behaviors of the empirical loss $\widehat{\mathcal{L}}_U$, and establish an exponential concentration inequality for $\widehat{\mathcal{L}}_U$ under an exponential rate of the β -mixing condition.

Theorem 4.2. For any sparsity parameter $\lambda < \infty$ and $\epsilon > 0$, if Assumptions 1-2 and S.1-S.2 hold, we have ϵ -divergence of $|\widehat{\mathcal{L}}_U - \mathcal{L}_U|$ bounded in probability for sufficiently large T and n , that is

$$\mathbb{P}\left(|\widehat{\mathcal{L}}_U - \mathcal{L}_U| > \epsilon\right) \leq 2 \left[\exp\left(-\frac{c_1(T\epsilon^2/4 - \epsilon c_0 U_{\max}^2 \sqrt{T} + c_0^2 U_{\max}^4)}{U_{\max}^2(\epsilon/2 - c_0 U_{\max}^2/\sqrt{T}) \log T \log \log T + U_{\max}^4}\right) + \exp\left(-\frac{n\epsilon^2}{2U_{\max}^4}\right) \right],$$

where c_0, c_1 are some constants depending on δ_1 , respectively; and

$$U_{\max} := \left| \frac{2R_{\max}}{1-\gamma} + \frac{3\lambda}{2} - \min\left\{\frac{-R_{\max}}{1-\gamma}, 0\right\} \right| \vee \left| \frac{-3R_{\max}}{1-\gamma} - 2\lambda - \frac{\lambda}{2(1-\gamma)} \right|.$$

Theorem 4.2 shows that $\widehat{\mathcal{L}}_U$ is a consistent estimator for the loss \mathcal{L}_U with a high probability at an exponential rate. The concentration bound is sharper than the bound established in Borisov and Volodko (2009). Here, we require an exponential decaying mixing rate, which is standard in the literature of deriving concentration inequalities for weakly dependent data (Borisov and

Volodko, 2009; Merlevède et al., 2011). It should be possible to relax this mixing condition to a polynomial-decay rate of β -mixing with imposing an additional exponential α -mixing condition. However, that is out of the scope of this paper.

We denote $\mathcal{L}_U^* = \inf_{\{V_\lambda, \pi_\lambda, \Psi, \psi\}} \mathcal{L}_U(V_\lambda, \pi_\lambda, \Psi, \psi)$ as the minimal risk, also called Bayes risk (Bartlett et al., 2006). Then, we define the empirical risk minimizer of $\widehat{\mathcal{L}}_U$ as

$$(\widehat{V}_\lambda^{\theta_1}, \widehat{\pi}_\lambda^{\theta_2}, \widehat{\Psi}^\xi, \widehat{\psi}^{\theta_3}) = \arg \min_{\{V_\lambda^{\theta_1}, \pi_\lambda^{\theta_2}, \Psi^\xi, \psi^{\theta_3}\} \in \Theta_1 \times \Theta_2 \times \Xi \times \Theta_3} \widehat{\mathcal{L}}_U(V_\lambda^{\theta_1}, \pi_\lambda^{\theta_2}, \Psi^\xi, \psi^{\theta_3}),$$

where Θ_1, Θ_2, Ξ and Θ_3 are function spaces corresponding to $V_\lambda^{\theta_1}, \pi_\lambda^{\theta_2}, \Psi^\xi$ and ψ^{θ_3} , respectively. Recall that $(V_\lambda^*, \pi_\lambda^*)$ are the optimal value function and policy, and $\{\Psi, \psi\} = \inf_{\{\Psi, \psi\}} \mathcal{L}_U(V_\lambda^*, \pi_\lambda^*, \Psi, \psi)$ are the corresponding Lagrange functions minimizing the risk \mathcal{L}_U , then the minimal risk \mathcal{L}_U^* is equivalent to $\mathcal{L}_U(V_\lambda^*, \pi_\lambda^*, \Psi, \psi)$. In Theorem 4.3, we establish the excess risk bound and derive a convergence rate of $\mathcal{L}_U(\widehat{V}_\lambda^{\theta_1}, \widehat{\pi}_\lambda^{\theta_2}, \widehat{\Psi}^\xi, \widehat{\psi}^{\theta_3}) - \mathcal{L}^*$. The following assumptions on the function space capacity is needed in order to develop the theoretical results .

Assumption 3. *There exists a constant $\mathbf{C} > 0$, and $q \in (0, 2)$ such that for any $\varepsilon > 0$, $0 < \lambda \leq \lambda_{\max} < \infty$, $R_{\max}/(1 - \gamma) < \infty$, the following condition on metric entropy is satisfied,*

$$\begin{aligned} & \log \left(\max \left\{ \mathcal{N}(\varepsilon, \Theta_1, \|\cdot\|_\infty), \mathcal{N}(\varepsilon, \Theta_2, \|\cdot\|_\infty), \mathcal{N}(\varepsilon, \Xi, \|\cdot\|_\infty), \mathcal{N}(\varepsilon, \Theta_3, \|\cdot\|_\infty) \right\} \right) \\ & \leq \mathbf{C} \left(\frac{\max\{\lambda_{\max}, R_{\max}/(1 - \gamma) + \lambda_{\max}/2, 1/2\}}{\varepsilon} \right)^q, \end{aligned}$$

where $\|\cdot\|$ denotes the supreme norm and $(V_\lambda^{\theta_1}, \pi_\lambda^{\theta_2}, \Psi^\xi, \psi^{\theta_3}) \in \Theta_1 \times \Theta_2 \times \Xi \times \Theta_3$.

Assumption 3 characterizes the complexity of the function spaces. In general, it is more difficult to estimate the functions as ε decreases. This assumption is satisfied in the function spaces such as the RKHS and Sobolev space (Geer and van de Geer, 2000; Steinwart and Christmann, 2008). Moreover, we compare this assumption with the assumption 3 in (Antos et al., 2008) which considers parametric function spaces with finite effective dimension $D_{\mathcal{F}}$. Their assumption is equivalent to assuming $\log \mathcal{N}(\varepsilon, \Theta_1, \|\cdot\|) \leq D_{\mathcal{F}} \log(1/\varepsilon)$, which is only able to account for the capacity of the finite dimension space. In contrast, our assumption is more general and allows our theorems can be applied to both finite and infinite dimension space.

Theorem 4.3. *Under Assumptions 1-3 and S.1-S.4, for any $\delta \in (0, 1]$, $q \in (0, 2)$ and $\lambda \in (0, \lambda_{\max})$, then the excess risk $\mathcal{E}(\mathcal{L}_U) := \mathcal{L}_U(\widehat{V}_\lambda^{\theta_1}, \widehat{\pi}_\lambda^{\theta_2}, \widehat{\Psi}^\xi, \widehat{\psi}^{\theta_3}) - \mathcal{L}^*$ is upper bounded with probability at least $1 - \delta$, that is*

$$\begin{aligned} \mathcal{E}(\mathcal{L}_U) \leq & c_2(n^{-1} + n^{-\frac{1}{2+q}}) + J_1(\delta) \left(\frac{\log \log \left(-2^{-\frac{\delta_1}{1+\delta_1}} c_3^{\delta_1} T^{\frac{\delta_1}{1+\delta_1}} \right)}{T} \right)^{1/2} \\ & + J_2(\delta) \left(T^{\frac{1-\delta_1}{(\delta_1+1)(2+q)}} \right) + J_3(\delta) \left(\frac{\log \left(c_4 T^{\frac{2}{1+\delta_1}} \right)}{T^{\frac{1}{2+q}}} \right)^{1/2}. \end{aligned} \quad (4.1)$$

If constants and logarithmic terms are omitted, the excess risk can be simplified asymptotically to

$$\mathcal{E}(\mathcal{L}_U) \asymp \mathcal{O} \left(\left(n \wedge T^{\frac{\delta_1-1}{\delta_1+1}} \right)^{-\frac{1}{2+q}} \wedge \left(T^{-1} \log \log (T^{\frac{\delta_1}{1+\delta_1}}) \right)^{\frac{1}{2}} \right),$$

where $J_1(\delta), J_2(\delta), J_3(\delta)$ are functions of $\delta, \delta_1, \mathbf{C}, c_3, q, U_{\max}, \lambda_{\max}, R_{\max}, \gamma, \zeta$, and c_2, c_3, c_4 which are some constants depending on $\delta_1, \mathbf{C}, q, U_{\max}, \lambda_{\max}, R_{\max}, \gamma$.

The first two terms in (4.1) control the statistical error from the empirical estimation over n i.i.d. trajectories. The third and fourth terms bound the trajectory-based stochastic error from the variability inherent in weakly dependent within-trajectory samples. It observes that the third and fourth terms depends on the complexity of the function spaces $\Theta_1 \times \Theta_2 \times \Xi \times \Theta_3$. In addition, the last term is a reminder term due to using *block devices* in dealing with the sample dependency. In general, this reminder term converges to zero much faster than other main terms, especially when the sample dependency is weak in that δ_1 is large. Hence, the reminder term does not affect the established convergence rate.

Theorem 4.3 provides a more powerful result than just a consistency of estimation as it establishes a finite-sample upper bound guarantee for the risk. In particular, if the process $\{(S^t, A^t)\}_{t \geq 1}$ forgets its past history sufficiently fast, i.e. $\delta_1 \rightarrow \infty$, then $T^{(\delta_1-1)/(\delta_1+1)}$ and $T^{\delta_1/(1+\delta_1)}$ both converge to T . Since the term $\log \log (T^{\delta_1/(1+\delta_1)})$ is a negligible to $\mathcal{O}(T^{-1})$, we may achieve the optimal sample complexity upper bound $\mathcal{O}(n^{-1/(2+q)})$ if T is the same order of n . In particular, when the state space \mathcal{S} is an open Euclidean ball in \mathbb{R}^d , and for a second-order Sobolev space $\mathbb{W}^{j,2}$

with $j > d/2$, one can choose $q = d/j$ to obtain the risk upper bound of the rate $\mathcal{O}(n^{-d/2(j+d)})$. Besides establishing the risk bound in infinite dimensional function spaces, Theorem 4.3 can also be applied for the finite dimensional function spaces. That is, Theorem 4.3 recovers the best upper error bound $n^{-1/2}$ when $q \rightarrow 0$, .

In the following, we provide a finite sample upper bound on the performance error of the estimated optimal value function. Let $K(\cdot, \cdot)$ be a continuous integral strictly positive definite kernel on the compact metric space $\mathcal{S} \times \mathcal{A}$, and there exists an orthonormal basis e_1, e_2, \dots , for $L^2(\mathcal{S} \times \mathcal{A})$. Also, we let $\kappa_1, \kappa_2, \dots$, be corresponding eigenvalues such that $K(\{s, a\}, \{\tilde{s}, \tilde{a}\}) = \sum_{j=1}^{\infty} \kappa_j e_j(\{s, a\}) e_j(\{\tilde{s}, \tilde{a}\})$, where $\{s, a\}, \{\tilde{s}, \tilde{a}\} \in \mathcal{S} \times \mathcal{A}$. Denote $\mathcal{K}_{\text{inf}}^\lambda := \inf\{\sup_{s \in \mathcal{S}} \mathcal{K}(s), |\mathcal{A}|\}$ as the maximum cardinality of the support set \mathcal{K} with respect to λ ; and $\|f\|_{L^2}$ denotes the L^2 norm that $\sqrt{\int f^2(s) dd_{\pi_b}(s)}$ for the observed data distribution d_{π_b} over \mathcal{S} .

Theorem 4.4. *Under Assumptions 1-3 and S.1-S.4, for $\lambda \in (0, \lambda_{\max})$ and the finite minimum eigenvalue $\kappa_{\min} = \min\{\kappa_1, \kappa_2, \dots\} < \infty$, the performance error between the estimated optimal value function $\widehat{V}_\lambda^{\theta_1}$ with respect to the proximal Bellman operator \mathcal{B}_λ and the optimal value function V^* with respect to the standard Bellman operator \mathcal{B} is upper bounded by*

$$\|\widehat{V}_\lambda^{\theta_1} - V^*\|_{L^2}^2 \leq \frac{c_5 \mathcal{E}(\mathcal{L}_U)}{\kappa_{\min}(1-\gamma)^2} + \frac{c_6 \lambda^2}{(1-\gamma)^2} |\mathcal{K}_{\text{inf}}^\lambda| + \frac{c_7 \lambda^2 |\mathcal{K}_{\text{inf}}^\lambda| + \lambda^2 c_8}{(1-\gamma)^2 |\mathcal{K}_{\text{inf}}^\lambda|},$$

where c_5, c_6, c_7, c_8 are some terms of $\delta_1, \mathbf{C}, c_2, c_3, c_4, J_1(\delta), J_3(\delta), q, U_{\max}, \zeta, \lambda_{\max}, R_{\max}, \gamma$ in which $c_6 > c_7$.

The above bound provides some insights into the performance of the proposed method. Specifically, under the regularity conditions, the proposed method is a consistent algorithm. As the number of samples and the length of trajectory increase, the estimated optimal value function $\widehat{V}_\lambda^{\theta_1}$ converges to the optimal value function V^* asymptotically. Note that the last two terms vanish to zero as $\lambda \rightarrow 0$; this implies that no smoothing bias is involved in the finite sample bound of $\|\widehat{V}_\lambda^{\theta_1} - V^*\|_{L^2}^2$. Moreover, combined with the sample bound for an excess risk $\mathcal{E}(\mathcal{L}_U)$ in Theorem 4.3, Theorem 4.4 indicates that the behavior of the upper bound as a function of samples $\mathcal{O}(n^{-1/(2+q)})$ is the best. In general, a large λ increases the smoothing error but decreases the approximation error as the solution function space is better behaved due to stronger

smoothness. However, the approximation error is not reflected in our sample bound because we make the zero approximation error assumption in Assumption S.4.

5 Implementation and Algorithm

In general, the functions $(V_\lambda, \pi_\lambda, \Psi, \psi)$ are required to be parameterized by a class of models for practical implementations. One may parameterize $(V_\lambda, \pi_\lambda, \Psi, \psi)$ by $\{V_\lambda(\cdot; \beta), \pi_\lambda(\cdot; \theta), \Psi(\cdot; \omega), \psi(\cdot; \xi)\}$, where $(\theta, \beta, \omega, \xi)$ are associated parameters. Note that the policy (actor) $\pi_\lambda(\cdot; \theta)$ and the value function (critic) $V_\lambda(\cdot; \beta)$ are separately represented by the two sets of parameters (θ, β) . This parametrization representation is aligned with the *actor-critic* paradigm in estimating the policy, which requires assistance and evaluation from the critic (Mnih et al., 2016). In our algorithm development, we introduce a unified *actor-critic* paradigm where the actor itself can play a critic role such that the actor can be self-supervised during the training process. We allow both V_λ and π_λ to be represented in terms of Q_λ based on the connections in (3.3) and (3.5), respectively. In other words, it is sufficient to only parametrize Q_λ for V_λ and π_λ . Specifically, if we parametrize Q_λ by $Q_\lambda(\cdot; \theta)$, then $\{V_\lambda, \pi_\lambda\}$ can be parametrized by the same set of parameter θ , i.e. $\{V_\lambda(\cdot; \theta), \pi_\lambda(\cdot; \theta)\}$. One advantage of the new diagram is to reduce the parameter space, from two sets of parameters to one set, and hence relaxing the computational intensity. Another key advantage is that the new diagram only need to track the target policy $\pi_\lambda(\cdot; \theta)$ instead of tracking the non-stationary target V_λ which usually results in convergence issues.

For any state-action pair (s, a) , we follow the new unified *actor-critic* framework to approximate $Q_\lambda(s, a)$ using basis function approximations. The state-action function $Q_\lambda(s, a; \theta)$ is represented by a linear combination of basis functions $\theta^T \varphi(s, a)$, where θ is a p_Q -dimensional weight vector and $\varphi(s, a)$ is a column vector of non-linear basis functions computed at (s, a) . For $m = p_Q/|\mathcal{A}|$, the vector $\varphi(s, a)$ sets the basis function value $\varphi(s) = (\varphi_1(s), \varphi_2(s), \dots, \varphi_m(s))$ in the corresponding slot for a specific action a , while the values of basis function for the rest of

the actions are set to be zero. That is

$$\varphi(s, a_1) = \begin{bmatrix} \varphi_1(s) \\ \dots \\ \varphi_m(s) \\ \mathbf{0}_{m(|\mathcal{A}|-1) \times 1} \end{bmatrix}, \dots, \varphi(s, a_k) = \begin{bmatrix} \mathbf{0}_{m(k-1) \times 1} \\ \varphi_1(s) \\ \dots \\ \varphi_m(s) \\ \mathbf{0}_{m(|\mathcal{A}|-2) \times 1} \end{bmatrix}, \dots, \varphi(s, a_{|\mathcal{A}|}) = \begin{bmatrix} \mathbf{0}_{m(|\mathcal{A}|-1) \times 1} \\ \varphi_1(s) \\ \dots \\ \varphi_m(s) \end{bmatrix},$$

where $\mathbf{0}$ is a zero vector. Similarly, we model the two Lagrangian functions as $\Psi(s; \omega) = \omega^\top \varphi(s)$ and $\psi(a, s; \xi) = \xi^\top \varphi(s, a)$. The flexibility of these working models can be achieved by selecting different $\varphi(\cdot)$, such as B-splines, radial basis or Fourier basis functions. Also note that $Q_\lambda(s, a; \theta)$ can be parametrized by a non-linear approximation architecture and the optimization convergence is guaranteed in the pT-learning framework.

In the following, we reformulate the empirical risk minimization (3.14) to a nonlinear programming problem for which the objective is converted to a quadratic term with a nonlinear equality constraint and a nonlinear inequality constraint,

$$\begin{aligned} \min_{\theta, \omega, \xi} \widehat{\mathcal{L}}_U(\theta, \omega, \xi) &= \frac{\zeta}{n} \sum_{i=1}^n (D_i(\theta) - P_i(\theta) - Z_i(\omega) + W_i(\xi))^\top \Omega_i (D_i(\theta) - P_i(\theta) - Z_i(\omega) + W_i(\xi)) \\ \text{s.t. } P_i(\theta) \odot W_i(\xi) &= 0, \quad -\frac{\lambda}{2} \cdot \mathbf{1} \leq Z_i(\omega) \leq \mathbf{0} \quad \text{for } i = 1, \dots, n, \end{aligned} \quad (5.1)$$

where \odot denotes the Hadamard product and $\Omega_i \in \mathbb{R}^{T \times T}$ is the weighting matrix with $\{\Omega_i\}_{jk} = \{2(K(\{S_i^j, A_i^j\}, \{S_i^k, A_i^k\}) - \mathbb{1}(j = k)) / T(T-1)\}_{jk}$. The details of the remaining terms $D_i(\theta)$, $P_i(\theta)$, $Z_i(\omega)$ and $W_i(\xi)$ are provided in the Appendix.

To solve this quadratic programming problem with non-linearity constraints, one may consider applying sequential quadratic programming (Fletcher, 2010) to optimize the objective function with linearized constraints. However, this requires several derivatives which are required to be solved analytically before iteration. Therefore, it can be quite cumbersome in practical implementations. Another approach is to apply exterior penalty methods (Boyd et al., 2004), which convert a constrained problem to a series of unconstrained optimization problems. However, the size of constraints is $\mathcal{O}(|\mathcal{S}||\mathcal{A}|)$, and thus the computation is intensive if either $|\mathcal{S}|$ or $|\mathcal{A}|$ is large.

Alternatively, we propose a computationally more efficient algorithm, solving an uncon-

strained optimization via imposing certain restrictions on the representation of $\{Z_i(\omega), W_i(\xi)\}$ such that the two Lagrangian functions satisfy the constraints automatically. Although this re-parametrization may sacrifice certain model flexibility, it gains computational advantages as it solves a simpler quadratic optimization problem. More specifically, we parametrize $Z_i(\omega)$ by flipping a sigmoid function:

$$Z_i(\omega) = \left\{ \frac{-\lambda/2}{1 + \exp(-k_0(\omega^\top S_i^j - b_0))} \right\}_{j=1}^T \in [-\lambda/2, 0]^{T \times 1}, \quad (5.2)$$

where b_0 is the sigmoid's midpoint and k_0 is the logistic growth rate. Obviously, the first inequality constraint $-\lambda/2 \cdot \mathbf{1} \leq Z_i(\omega) \leq \mathbf{0}$ is automatically satisfied under this parameterization. Observe that the j -th element of $P_i(\theta)$ satisfies $P_{ij}(\theta) > 0$ when $a \in \mathcal{K}(S_i^j)$, and $P_{ij}(\theta) = 0$ otherwise. Therefore, we can further reduce our parameter space via modeling $W_i(\xi)$ as a function of θ instead of ξ . That is,

$$W_i(\theta) = \left\{ \left(\sum_{a \in \mathcal{K}(S_i^j)} \theta^\top \varphi(S_i^j, a) - \lambda - \theta^\top \varphi(S_i^j, A_i^j) |\mathcal{K}(S_i^j)| \right)^+ \right\}_{j=1}^T \in \mathbb{R}^{T \times 1}, \quad (5.3)$$

where the equality constraint $W_i(\theta) \odot P_i(\theta) = 0$ is always satisfied. The auxiliary parameter ξ is replaced by θ in the optimization, and hence the computational complexity is further reduced.

Algorithm 1 pT-Learning with Stochastic Gradient Descent

- 1: **Input** observed data \mathcal{D}_n as the transition pairs format $\{(S_i^t, A_i^t, R_i^t, S_i^{t+1}) : t = 1, \dots, T\}_{i=1}^n$.
- 2: **Initialize** the primary and auxiliary parameters $(\theta, \omega) = (\theta_0, \omega_0)$, the mini-batch size n_0 , the learning rates $\alpha_\theta = \alpha_\theta^0, \alpha_\omega = \alpha_\omega^0$, the scale parameter $\zeta = \zeta_0$, the adjustment factors $(\kappa_e, \kappa_\pi, \kappa_\alpha)$, the sparsity parameter $\lambda = \lambda_0$, the kernel bandwidth $bw = bw_0$, and the stopping criterion ε .
- 3: **For** $k = 1$ to $k = \text{max.iter}$
- 4: Randomly sample a mini-batch $\{(S_i^t, A_i^t, R_i^t, S_i^{t+1}) : t = 1, \dots, T\}_{i=1}^{n_0}$.
- 5: Compute the stochastic gradient with respect to θ as

$$\bar{\Delta}_\theta = \frac{\zeta_0}{n_0} \sum_{i=1}^{n_0} [D_i(\theta) - P_i(\theta) + W_i(\theta)]^\top \Omega_i [\kappa_e \nabla_\theta D_i(\theta) + \kappa_\pi \nabla_\theta P_i(\theta) + \kappa_\alpha \nabla_\theta W_i(\theta)].$$

- 6: Compute the stochastic gradient w.r.t. ω as $\bar{\Delta}_\omega = \frac{\zeta_0}{n_0} \sum_{i=1}^{n_0} Z_i(\theta)^\top \Omega_i \nabla_\theta Z_i(\theta)$.
 - 7: Decay the learning rate $\alpha_\theta^k = \mathcal{O}(k^{-1/2}), \alpha_\omega^k = \mathcal{O}(k^{-1})$.
 - 8: Update the parameters of interest as $\theta^k \leftarrow \theta^{k-1} - \alpha_\theta^k \bar{\Delta}_\theta, \omega^k \leftarrow \omega^{k-1} - \alpha_\omega^k \bar{\Delta}_\omega$.
 - 9: Stop if $\|\theta^k - \theta^{k-1}\| \leq \varepsilon$.
 - 10: **Return** $\hat{\theta} = \theta^k$.
-

The minimization of $\widehat{\mathcal{L}}_U(\theta, \omega)$ requires $\mathcal{O}(nqT^2)$ complexity in calculating the exact gradients. Here, we implement a stochastic gradient descent (SGD) algorithm, where the training is on mini-batch datasets and is faster than a vanilla gradient descent or BFGS algorithm. We summarize the details of the proposed algorithm in Algorithm 1. Note that $P_i(\theta)$ is continuously differentiable except at the splitting boundary where the support set $\{\mathcal{K}(S_i^j)\}_{j=1}^T$ changes. In addition, the time complexity of calculating the gradient requires $\mathcal{O}(|\mathcal{A}| \log(|\mathcal{A}|)Tqn)$ by a naive sorting algorithm, and we can further improve the time complexity to $\mathcal{O}(|\mathcal{A}|Tqn)$ by utilizing the bucket-sorting algorithm (Blum et al., 1973).

6 Simulation Studies

We conduct two numerical experiments to evaluate the finite sample performance of the proposed method. In the first experiment, we consider a binary treatment setting following a benchmark generative model (Luckett et al., 2020; Liao et al., 2020). In the second experiment, we mimic an mHealth cohort study aiming to deliver personalized interventions with 12 choices for managing an individual’s glucose level. In both experiments, we compare our approach to state-of-the-art methods including linear, polynomial and Gaussian V-learning (Luckett et al., 2020), and GMM-Qlearning (Ertefaie and Strawderman, 2018). The proposed method is implemented and available in our proximalDTR R package.

In the first example, we let the current state $S_i^t = (S_{i,1}^t, S_{i,2}^t)^T$ be a two-dimensional vector and the current action $A_i^t \in \{1, 0\}$. The next state S_i^{t+1} is generated according to $S_{i,1}^{t+1} = (3/4)(2A_i^t - 1)S_{i,1}^t + (1/4)S_{i,1}^t S_{i,2}^t + \epsilon_{i,1}^t$ and $S_{i,2}^{t+1} = (3/4)(1 - 2A_i^t)S_{i,2}^t + (1/4)S_{i,1}^t S_{i,2}^t + \epsilon_{i,2}^t$, where the random noises $\epsilon_{i,1}^{t+1}$ and $\epsilon_{i,2}^{t+1}$ follow an independent Gaussian distribution $N(0, 0.5^2)$. Note that assigning $A_i^t = 1$ imposes a positive effect on $S_{i,1}^{t+1}$ but has a negative effect on $S_{i,2}^{t+1}$. We define a nonlinear utility function $u(S_i^{t+1}, A_i^{t+1}, S_i^t)$ such that

$$R_i^t = u(S_i^{t+1}, S_i^t, A_i^t) = (1/4)(S_{i,1}^{t+1})^3 + 2S_{i,1}^{t+1} + (1/2)(S_{i,2}^{t+1})^3 + S_{i,1}^{t+1} + (1/4)(2A_i^t - 1).$$

The initial state S_i^1 follows a Gaussian distribution $N(0, I_{2 \times 2})$ and A_i^1 is randomly assigned with

an equal probability for each treatment arm as in micro-randomized trials.

We consider different scenarios in which the number of patients $n = \{50, 100\}$ and the follow-up time length $T = \{24, 36, 48\}$. The discount factor γ is set to be 0.9, focusing on long-term benefits. To specify the basis function $\varphi(s)$ mentioned in Section 5, we consider a cubic spline containing six knots located in equal space of interval $[0, 1]$, and then apply it to the state variables normalized between 0 and 1.

The objective function $\widehat{\mathcal{L}}_U(\theta, \omega)$ may not be convex with respect to both θ and ω . Therefore, we adopt a multiple initialization method to determine an appropriate initial point. Specifically, we choose the initial point with the smallest objective value among 200 randomly generated initial points. To determine the sparsity parameter λ , we select the optimal one which maximizes the lower bound of the empirical discounted sum of utilities, $\widehat{\lambda} = \arg \max_{\lambda} \mathbb{P}_n \widehat{V}_{\lambda}(S_i^1; \widehat{\theta}) - \lambda \phi(0)/(1 - \gamma)$, where S_i^1 is the observed initial state of the i -th subject.

To evaluate the model performance, we use the mean utility under the estimated policy as an evaluation criterion. Specifically, after obtaining the estimated policy, we simulate 100 independent individual patients following this estimated policy over 100 stages, and calculate the mean utility. Therefore, a larger value of the mean utility indicates a better policy. In Table 1, we report the average and standard deviations of the mean utilities over 50 simulation runs.

Table 1: Example 1: The average and standard deviation (in parentheses) of the mean utilities under the estimated optimal policy based on 50 simulation runs.

n	T	Proposed	GMM-QL	Linear VL	Polynomial VL	Gaussian VL	Observed
50	24	0.4036(0.071)	0.0874(0.242)	0.2718(0.033)	0.2753(0.036)	0.2602(0.021)	-0.0213
	36	0.4020(0.069)	0.0782(0.237)	0.2605(0.024)	0.2603(0.024)	0.2582(0.021)	0.0113
	48	0.4053(0.041)	0.0977(0.236)	0.2595(0.022)	0.2594(0.022)	0.2578(0.020)	-0.0393
100	24	0.4115(0.029)	0.0894(0.247)	0.2634(0.025)	0.2642(0.023)	0.2568(0.012)	0.0291
	36	0.4079(0.036)	0.0825(0.259)	0.2578(0.014)	0.2576(0.013)	0.2563(0.012)	-0.0241
	48	0.4057(0.033)	0.1028(0.249)	0.2565(0.011)	0.2567(0.012)	0.2563(0.011)	-0.0072

Table 1 shows that the proposed method outperforms the competing methods in all scenarios. When the sample size $n = 100$ and the number of stages $T = 24$, compared to the baseline, i.e., the observed mean utility, the proposed method improves 0.3824 while the polynomial V-learning and the GMM-Qlearning only improve 0.2351 and 0.0603, respectively. This is mainly because

the proposed method does not impose restrictions on the class of policies as in V-learning. Also, the induced policy can be automatically adjusted between deterministic and stochastic policy models. In addition, the proposed method utilizes the smoothed proximal Bellman operator, and thus avoids discontinuity and instability. Moreover, the proposed method has advantages in off-policy training due to utilizing the proximal temporal consistency property. In contrast, GMM-Qlearning tends to solve the hard Bellman optimality equation, which could be difficult without large amounts of samples. Computational-wise, the pT-Learning approach requires less than one minute to converge under $n = 100$ and $T = 48$, while Gaussian V-learning takes more than 10 minutes for any single experiment.

In the second example, we simulate cohorts of patients with type 1 diabetes to mimic the mobile health study (Maahs et al., 2012). The study aims to achieve long-term glycemic control and maintain the rest of the health index in the desired ranges. Specifically, our hypothetical mHealth study targets to searching the optimal policy for suggesting multi-channel interventions; the insulin injection (IN), physical activity (PA), and dietary intake (DI), to control the blood glucose (BG) level in the desired range while maintaining healthy levels of Adiponectin (AD) and blood pressure (BP) (Fidler et al., 2011). Hence, the immediate utility R_i^t is defined by a weighted summation of patients' health status as following,

$$\begin{aligned} R_i^t = & \alpha_1 \mathbb{1}(70 \leq \text{BG}_i^{t+1} \leq 120) + \alpha_2 \mathbb{1}(\text{BG}_i^{t+1} < 70 \text{ or } \text{BG}_i^{t+1} > 150) + \alpha_3 \mathbb{1}(120 \leq \text{BG}_i^{t+1} \leq 150) \\ & + \alpha_4 \mathbb{1}(5 \leq \text{AD}_i^{t+1} \leq 23) + \alpha_5 \mathbb{1}(\text{AD}_i^{t+1} < 5 \text{ or } \text{AD}_i^{t+1} > 23) + \alpha_6 \mathbb{1}(66 \leq \text{BP}_i^{t+1} \leq 80) \\ & + \alpha_7 \mathbb{1}(\text{BP}_i^{t+1} < 66 \text{ or } \text{BP}_i^{t+1} > 80), \end{aligned}$$

where $(\alpha_1, \dots, \alpha_7) = (3, -3, -1, 2, -1, 2, -1)$ are weights reflecting the clinical consequences. The value of the utility varies from 3 to -6 , and a large value of utility is preferred.

The patients are assigned treatment from a combination of the insulin injections (Yes/No), physical activity (No/Moderate/Strong) and dietary intake (Yes/No). Note that there are total 12 different treatment choices, i.e., $\mathcal{A} = \{1, \dots, 12\}$. The details of the 12 different treatment combinations are enumerated in the Appendix. At each stage, the treatment $A_i^t \in \mathcal{A}$ is randomly assigned with equal probability for each treatment arm. The patient's state $(\text{BG}_i^t, \text{AD}_i^t, \text{BP}_i^t)$

evolves according to the given dynamic model: $BG_i^{t+1} = \gamma_{11}\mu_{BG} + \gamma_{12}BG_i^t - \gamma_{13}AD_i^t + \mu_{1k}\mathbb{1}(A_i^t = k) + \epsilon_{1i}^{t+1}$; $AD_i^{t+1} = \gamma_{21}\mu_{AD} + \gamma_{22}AD_i^t + \gamma_{23}BG_i^t + \mu_{2k}\mathbb{1}(A_i^t = k) + \epsilon_{2i}^{t+1}$; $BP_i^{t+1} = \gamma_{31}\mu_{BP} + \gamma_{32}BP_i^t + \mu_{3k}\mathbb{1}(A_i^t = k) + \epsilon_{3i}^{t+1}$, where $\epsilon_{1i}, \epsilon_{2i}$ and ϵ_{3i} are individual-level Gaussian random noises. The details of this generative model are provided in the Appendix.

Table 2: Example 2 (mHealth study): The average and standard deviation (in parentheses) of the mean utilities under the estimated optimal policy based on 50 simulation runs.

n	T	Proposed	GMM-QL	Linear VL	Poly VL	Gauss VL	Observed
75	24	2.675(0.220)	1.542(1.206)	1.616(0.340)	1.780(1.004)	1.704(1.056)	1.485
	36	2.780(0.524)	1.592(1.348)	1.737(0.598)	1.895(0.812)	2.026(0.797)	1.483
100	24	2.824(0.268)	1.678(0.928)	1.561(0.317)	1.736(0.801)	1.850(0.508)	1.472
	36	2.871(0.430)	1.732(1.102)	1.684(0.300)	1.909(0.723)	1.910(0.612)	1.477

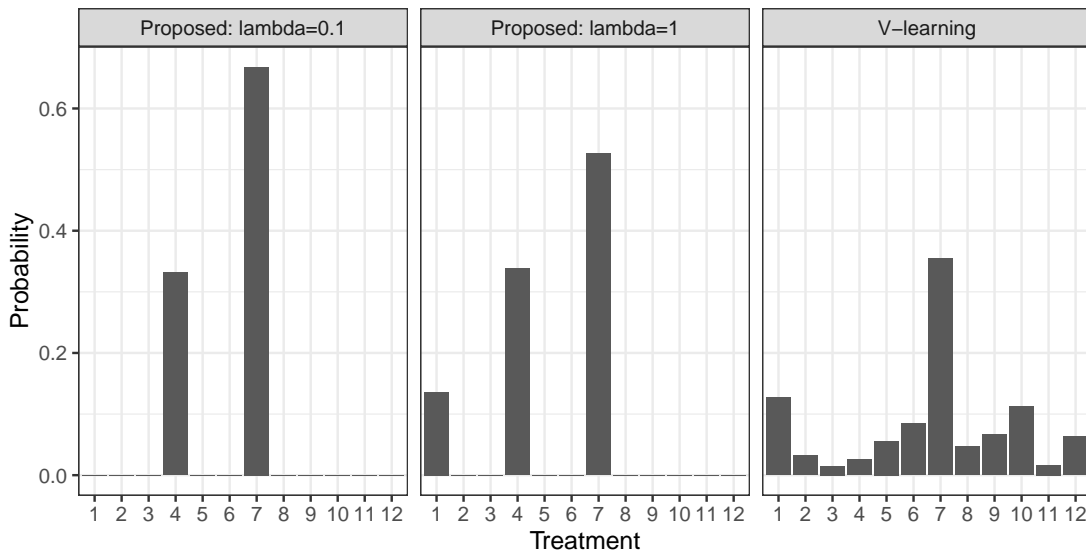


Figure 2: The estimated optimal policy distribution of pT-Learning and V-learning for one patient at a specific time point. The 7th treatment is the optimal treatment, and the 4th treatment is a near-optimal treatment; other treatments are sub-optimal or non-optimal treatments. The tuned optimal sparsity parameter is $\hat{\lambda} = 0.1$.

The cohort data is generated under different scenarios with a follow-up time length $T = \{24, 36\}$ and sample size $n = \{75, 100\}$. We use the same evaluation criterion as in Example 1 except that the testing set is simulated over 36 stages. The results are summarized in Table 2. The pT-Learning approach achieves the best performance. For example, when $n = 100$ and $T = 36$, pT-Learning achieves 50.3% and 65.8% improvements compared to Gaussian V-learning and

GMM-Qlearning, respectively. This is due to the sparse policy estimation of pT-Learning. For a better illustration, we visualize and compare the estimated policy distribution of pT-Learning and V-learning in Figure 2, where pT-Learning successfully allocates the optimal treatment by assigning large probabilities to the optimal treatment 7 and the near-optimal treatment 4. However, V-learning gives non-negligible probabilities to all non-optimal treatments, which leads to an inferior treatment recommendation. This is because GMM-Qlearning requires modeling the entire data-generating process, and hence produces a large over-estimation error. Worst of all, the GMM-Qlearning approach is designed to take the greedy action based on the fitted model. This again magnifies the over-estimation error and ultimately leads to a huge sub-optimality. In contrast, pT-Learning only requires modeling the optimal policy and optimal value function. Additionally, pT-Learning does not take a greedy action, but follows an adaptive and sparse stochastic policy model.

7 Application to Ohio Type 1 Diabetes Data

We apply the proposed method to two cohorts of individuals from the OhioT1DM dataset (Marling and Bunescu, 2020), which was used to study the long-term blood glucose management via the just-in-time interventions on the type 1 diabetes patients. Each cohort contains 6 individuals of age ranging within 20 to 60. All patients were on insulin pump therapy with continuous glucose monitoring (CGM) sensors, and the life-event data is collected via a mobile phone app. The physiological data of the first cohorts was collected by *Basis* sensor bands, and the second cohort used *Empatica* sensor bands. Specifically, the dataset includes CGM blood glucose levels measured per 5 minutes, insulin dose levels delivered to the patient, meal intakes, and corresponding carbohydrate estimates. Note that the heart rate measured per 5 minutes is available only for patients using the *Basis* sensor band (the first cohort), while the magnitude of acceleration aggregated per minute is only available with the *Empatica* sensor band (the second cohort). The data also include other features such as the self-reported times of work, sleep and stress, etc. Based on the preliminary investigation, each patient has distinct blood glucose dynamics.

Therefore, we follow the pre-processing strategy used in [Zhu et al. \(2020\)](#), and treat the data of each patient as a single dataset. Then we estimate the optimal policy by treating each day as an independent sample. For the first cohort, we consider a binary intervention setting, i.e., whether or not to provide the insulin injection; and for the second cohort, we study the individualized dose-finding problem by discretizing the continuous dose level into 14 disjoint intervals for intervention options. We compare the performance of pT-Learning with the same competing methods as in [Section 6](#).

We summarize the collected measurements over 60-min intervals such that the length of each trajectory is $T = 24$. After removing missing samples and outliers, each dataset contains $n = 15$ trajectories on average. For the first six patients who wore the *Basis* sensor band, the patient’s states at each stage include the average blood glucose levels $S_{i,1}^t$, the average heart rate $S_{i,2}^t$ and the total carbohydrates $S_{i,3}^t$ intake from time $t - 1$ and t . For others equipped with the *Empatica* sensor band, the states are the same as the first six patients, except that the average heart rate is substituted by the average magnitude of acceleration. Here, the utility is defined as the average of the index of glycemic control ([Rodbard, 2009](#)) between time $t - 1$ and t , measuring the health status of the patient’s glucose level. That is

$$R_i^t = -\frac{\mathbb{1}(S_{i,1}^t > 140)|S_{i,1}^t - 140|^{1.35} + \mathbb{1}(S_{i,1}^t < 80)(S_{i,1}^t - 80)^2}{30},$$

where R_i^t is non-positive and a larger value is preferred. Our goal is to maximize the expected discounted sum of utilities $\mathbb{E} \sum_{t \geq 1} \gamma^{t-1} R_i^t$. In the first cohort study, the treatment is binary, i.e. $A_i^t \in \{0, 1\}$. In the second study, we provide the optimal insulin dose suggestion via the uniform discretization of the continuous dose level, i.e., $A_i^t \in \{0 = A_{(1)} < \dots < A_{(14)} = \max(A)\}$.

Since the data-generating process is unknown, it is hard to use the mean utility under the estimated policy as the evaluation criterion as in [Section 6](#). Instead, we follow [Luckett et al. \(2020\)](#) to utilize the Monte Carlo approximation of the expected discounted sum of utilities for evaluating the model performance, i.e. $\mathbb{P}_n \widehat{V}(S_i^1)$, where S_i^1 is the initial state for the i th trajectory. In the competing methods, the quantity $\widehat{V}(\cdot)$ represents the estimated value function. In our method, we consider the lower bound of our estimated value function $\widehat{V}_\lambda(\cdot)$, i.e., $\mathbb{P}_n \widehat{V}_\lambda(S_i^1) - (1 -$

$\gamma)^{-1}\hat{\lambda}\phi(0)$, to mitigate the effects of the sparsity parameter $\hat{\lambda}$ on the utilities. This quantity can be also interpreted as the worst case of the discounted sum of utilities produced by pT-Learning. The discounted sum of observed utilities, i.e., $\mathbb{P}_n \sum_{t \geq 1} \gamma^{t-1} R_i^t$, is used as the baseline.

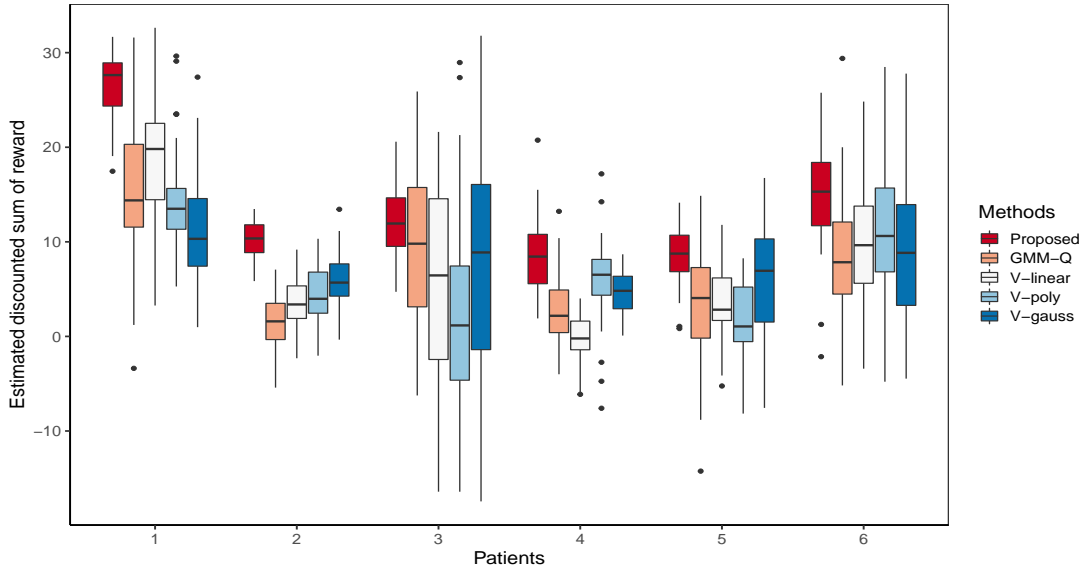


Figure 3: The first cohort of patients who wore the *Basis* sensor bands: Boxplots of the improvements on the Monto Carlo discounted sum of utilities relative to the baseline discounted sum of observed utilities. The results are summarized over 50 simulation runs when the treatment is binary and the discounted factor is $\gamma = 0.9$.

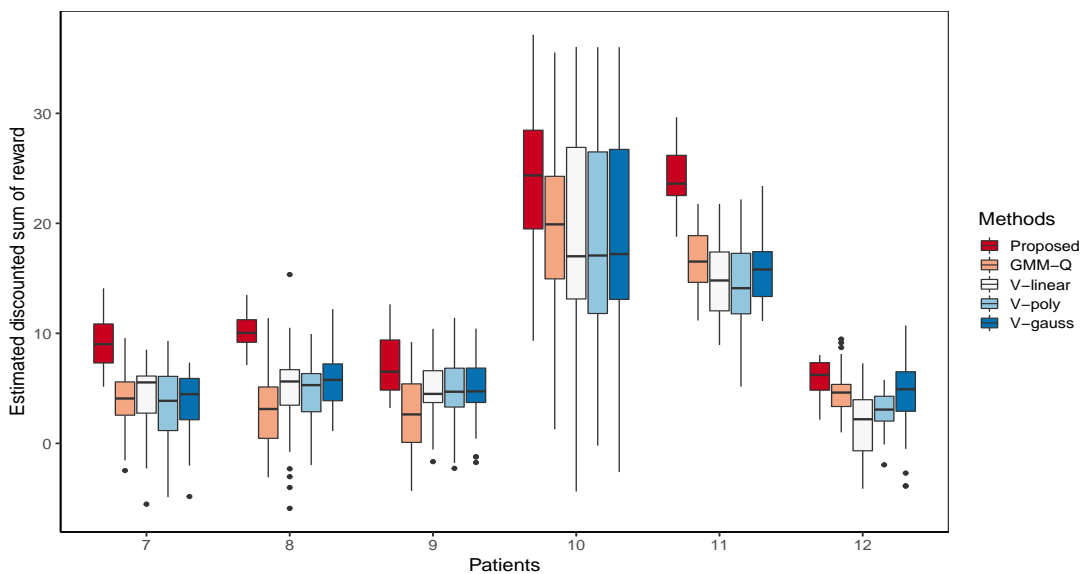


Figure 4: The second cohort of patients who wore the *Empatica* sensor bands: Boxplots of the improvements on the Monto Carlo discounted sum of utilities relative to the baseline discounted sum of observed utilities. The results are summarized over 50 simulation runs when the cardinality of the treatment $|\mathcal{A}| = 14$ and the discounted factor is $\gamma = 0.9$.

In our experiments, we choose two discount factors, $\gamma = 0.9$ and $\gamma = 0.8$. For the $\gamma = 0.9$ setting, the boxplots of the relative improvements of utilities are provided in Figure 3-4 for the first and second cohort data, respectively. Additional results are presented in the Appendix. Figure 3 indicates that pT-Learning achieves better improvements over competing methods across all patients. For example, for patient 1, the proposed method has 72.8% and 52.1% improvement rates compared to GMMQ-learning and the polynomial V-learning, respectively. This is mainly because pT-Learning does not impose restrictions on the class of policies and thus is more flexible. The standard deviation of the proposed method is the smallest among all approaches, reflecting that pT-Learning is relatively stable due to the smoothness property of the proximal Bellman operator and the implemented unified *actor-critic* framework. For the second cohort study with a large cardinality treatment space, pT-Learning substantially outperforms the competing methods in Figure 4. For the 7th patient, the improvement of pT-Learning to GMM-Qlearning and Gaussian V-learning attains 146.4% and 156.9%, respectively. This result shows that pT-Learning achieves high efficiency in the continuous treatment space, and our sparse policy estimation has a clear benefit with large numbers of treatment options.

8 Discussion

In this paper, we propose a novel proximal temporal consistency learning framework for estimating the optimal dynamic treatment regime in infinite time horizon settings. The constructed proximal Bellman operator directly leads to a smoothed Bellman optimality equation, while simultaneously inducing a sparse optimal policy. The proposed optimal policy distribution is not restricted to be either deterministic or stochastic, but can be adaptively adjusted. This property allows greater flexibility on the policy estimation, especially when the number of treatment options is large. To estimate the induced optimal policy, we propose a consistent minimax policy estimator, which avoids double sampling and can be easily optimized by a scalable and efficient stochastic gradient descent algorithm in off-policy data.

Several improvements and extensions are worth exploring in the future. First, we may extend

our algorithm to deal with strong temporal dependency. The idea of the experience-replay (Mnih et al., 2015) might be useful. It can be shown that the gradients calculated by the modified algorithm with experience replay are $1 - \mathcal{O}(n^{-1})$ -nearly independent. This breaks the data dependency if the number of trajectories is sufficiently large. The details of such an extension and theoretical justification are provided in the Appendix. Second, it is also useful to extend pT-Learning for the long-term average reward setting (Murphy et al., 2016). Third, developing statistical inference for quantifying uncertainty is also important. One might be interested in constructing confidence intervals for the estimated optimal policy and value function.

9 Supplementary Material

Online supplementary material includes the implementation details, additional numerical results, the connection between pT-learning and off-policy TD-algorithms, the pT-learning algorithm with experience-replay, additional assumptions, and the proof of all theorems, propositions and lemmas.

References

- Antos, A., Szepesvári, C., and Munos, R. (2008), “Learning near-optimal policies with Bellman-residual minimization based fitted policy iteration and a single sample path,” *Machine Learning*, 71, 89–129.
- Bach, F. (2017), “Breaking the curse of dimensionality with convex neural networks,” *The Journal of Machine Learning Research*, 18, 629–681.
- Baird, L. (1995), “Residual algorithms: Reinforcement learning with function approximation,” in *Machine Learning Proceedings 1995*, Elsevier, pp. 30–37.
- Bartlett, P. L., Jordan, M. I., and McAuliffe, J. D. (2006), “Convexity, classification, and risk bounds,” *Journal of the American Statistical Association*, 101, 138–156.

- Blum, M., Floyd, R. W., Pratt, V. R., Rivest, R. L., and Tarjan, R. E. (1973), “Time bounds for selection,” *J. Comput. Syst. Sci.*, 7, 448–461.
- Borisov, I. and Volodko, N. (2009), “Exponential inequalities for the distributions of canonical U-and V-statistics of dependent observations,” *Siberian Advances in Mathematics*, 19, 1–12.
- Boyd, S., Boyd, S. P., and Vandenberghe, L. (2004), *Convex Optimization*, Cambridge University Press.
- Chow, Y., Nachum, O., and Ghavamzadeh, M. (2018), “Path consistency learning in Tsallis entropy regularized MDPs,” in *International Conference on Machine Learning*, pp. 979–988.
- Dai, B., Shaw, A., Li, L., Xiao, L., He, N., Liu, Z., Chen, J., and Song, L. (2018), “SBEED: Convergent reinforcement learning with nonlinear function approximation,” in *International Conference on Machine Learning*, PMLR, pp. 1125–1134.
- Dann, C., Neumann, G., Peters, J., et al. (2014), “Policy evaluation with temporal differences: A survey and comparison,” *Journal of Machine Learning Research*, 15, 809–883.
- Ertefaie, A. and Strawderman, R. L. (2018), “Constructing dynamic treatment regimes over indefinite time horizons,” *Biometrika*, 105, 963–977.
- Farahmand, A.-m., Ghavamzadeh, M., Szepesvári, C., and Mannor, S. (2016), “Regularized policy iteration with nonparametric function spaces,” *The Journal of Machine Learning Research*, 17, 4809–4874.
- Fidler, C., Elmelund Christensen, T., and Gillard, S. (2011), “Hypoglycemia: An overview of fear of hypoglycemia, quality-of-life, and impact on costs,” *Journal of Medical Economics*, 14, 646–655.
- Fletcher, R. (2010), “The sequential quadratic programming method,” in *Nonlinear Optimization*, Springer, pp. 165–214.
- Geer, S. A. and van de Geer, S. (2000), *Empirical Processes in M-estimation*, vol. 6, Cambridge University Press.

- Gretton, A., Borgwardt, K. M., Rasch, M. J., Schölkopf, B., and Smola, A. (2012), “A kernel two-sample test,” *The Journal of Machine Learning Research*, 13, 723–773.
- Haarnoja, T., Zhou, A., Abbeel, P., and Levine, S. (2018), “Soft actor-critic: Off-policy maximum entropy deep reinforcement learning with a stochastic actor,” in *International Conference on Machine Learning*, PMLR, pp. 1861–1870.
- Hiriart-Urruty, J.-B. and Lemaréchal, C. (2012), *Fundamentals of Convex Analysis*, Springer Science & Business Media.
- Jiang, N. and Li, L. (2016), “Doubly robust off-policy value evaluation for reinforcement learning,” in *International Conference on Machine Learning*, PMLR, pp. 652–661.
- Korbel, J., Hanel, R., and Thurner, S. (2019), “Information geometric duality of ϕ -deformed exponential families,” *Entropy*, 21, 112.
- Kosorok, M. R. (2008), *Introduction to Empirical Processes and Semiparametric Inference*, Springer Science & Business Media.
- Lee, K., Choi, S., and Oh, S. (2018), “Sparse Markov decision processes with causal sparse Tsallis entropy regularization for reinforcement learning,” *IEEE Robotics and Automation Letters*, 3, 1466–1473.
- Liao, P., Klasnja, P., and Murphy, S. (2020), “Off-policy estimation of long-term average outcomes with applications to mobile health,” *Journal of the American Statistical Association*, 1–10.
- Luckett, D. J., Laber, E. B., Kahkoska, A. R., Maahs, D. M., Mayer-Davis, E., and Kosorok, M. R. (2020), “Estimating dynamic treatment regimes in mobile health using v-learning,” *Journal of the American Statistical Association*, 115, 692–706.
- Maahs, D. M., Mayer-Davis, E., Bishop, F. K., Wang, L., Mangan, M., and McMurray, R. G. (2012), “Outpatient assessment of determinants of glucose excursions in adolescents with type 1 diabetes: Proof of concept,” *Diabetes Technology & Therapeutics*, 14, 658–664.

- Maei, H. R., Szepesvári, C., Bhatnagar, S., and Sutton, R. S. (2010), “Toward off-policy learning control with function approximation,” in *Proceedings of the 27th International Conference on Machine Learning (ICML-10)*, pp. 719–726.
- Marling, C. and Bunesco, R. (2020), “The ohioT1DM dataset for blood glucose level prediction: Update 2020,” *KHD@ IJCAI*.
- Merlevède, F., Peligrad, M., and Rio, E. (2011), “A Bernstein type inequality and moderate deviations for weakly dependent sequences,” *Probability Theory and Related Fields*, 151, 435–474.
- Mnih, V., Badia, A. P., Mirza, M., Graves, A., Lillicrap, T., Harley, T., Silver, D., and Kavukcuoglu, K. (2016), “Asynchronous methods for deep reinforcement learning,” in *International Conference on Machine Learning*, pp. 1928–1937.
- Mnih, V., Kavukcuoglu, K., Silver, D., Rusu, A. A., Veness, J., Bellemare, M. G., Graves, A., Riedmiller, M., Fidjeland, A. K., Ostrovski, G., et al. (2015), “Human-level control through deep reinforcement learning,” *Nature*, 518, 529–533.
- Murphy, S. A. (2003), “Optimal dynamic treatment regimes,” *Journal of the Royal Statistical Society: Series B (Statistical Methodology)*, 65, 331–355.
- Murphy, S. A., Deng, Y., Laber, E. B., Maei, H. R., Sutton, R. S., and Witkiewitz, K. (2016), “A batch, off-policy, actor-critic algorithm for optimizing the average reward,” *arXiv preprint arXiv:1607.05047*.
- Nachum, O., Norouzi, M., Xu, K., and Schuurmans, D. (2017), “Bridging the gap between value and policy based reinforcement learning,” in *Advances in Neural Information Processing Systems*, pp. 2775–2785.
- (2018), “Trust-PCL: An Off-Policy Trust Region Method for Continuous Control,” in *International Conference on Learning Representations*.

- Nahum-Shani, I., Smith, S. N., Spring, B. J., Collins, L. M., Witkiewitz, K., Tewari, A., and Murphy, S. A. (2018), “Just-in-time adaptive interventions (JITAI) in mobile health: Key components and design principles for ongoing health behavior support,” *Annals of Behavioral Medicine*, 52, 446–462.
- Puterman, M. L. (2014), *Markov decision processes: discrete stochastic dynamic programming*, John Wiley & Sons.
- Rawlik, K., Toussaint, M., and Vijayakumar, S. (2013), “On stochastic optimal control and reinforcement learning by approximate inference,” in *Twenty-third International Joint Conference on Artificial Intelligence*.
- Rehg, J. M., Murphy, S. A., and Kumar, S. (2017), *Mobile Health*, Springer.
- Rodbard, D. (2009), “Interpretation of continuous glucose monitoring data: Glycemic variability and quality of glycemic control,” *Diabetes Technology & Therapeutics*, 11, S–55.
- Schulman, J., Chen, X., and Abbeel, P. (2017), “Equivalence between policy gradients and soft q-learning,” *arXiv preprint arXiv:1704.06440*.
- Shi, C., Fan, A., Song, R., and Lu, W. (2018), “High-dimensional A-learning for optimal dynamic treatment regimes,” *Annals of Statistics*, 46, 925–967.
- Shi, C., Zhang, S., Lu, W., and Song, R. (2020), “Statistical inference of the value function for reinforcement learning in infinite horizon settings,” *arXiv preprint arXiv:2001.04515*.
- Sim, I. (2019), “Mobile devices and health,” *New England Journal of Medicine*, 381, 956–968.
- Steinwart, I. and Christmann, A. (2008), *Support vector machines*, Springer Science & Business Media.
- Sutton, R. S. and Barto, A. G. (2018), *Reinforcement Learning: An Introduction*, MIT press.
- Uehara, M., Huang, J., and Jiang, N. (2020), “Minimax weight and q-function learning for off-policy evaluation,” in *International Conference on Machine Learning*, PMLR, pp. 9659–9668.

- Watkins, C. J. and Dayan, P. (1992), “Q-learning,” *Machine Learning*, 8, 279–292.
- Xu, Z., Laber, E., and Staicu, A.-M. (2020), “Latent-state models for precision medicine,” *arXiv preprint arXiv:2005.13001*.
- Yang, Q. and Van Stee, S. K. (2019), “The comparative effectiveness of mobile phone interventions in improving health outcomes: Meta-analytic review,” *JMIR mHealth and uHealth*, 7, e11244.
- Zhao, Y.-Q., Zeng, D., Laber, E. B., and Kosorok, M. R. (2015), “New statistical learning methods for estimating optimal dynamic treatment regimes,” *Journal of the American Statistical Association*, 110, 583–598.
- Zhu, L., Lu, W., and Song, R. (2020), “Causal Effect Estimation and Optimal Dose Suggestions in Mobile Health,” in *International Conference on Machine Learning*, PMLR, pp. 11588–11598.